MASTERARBEIT

Titel der Masterarbeit

„Effects of cJun and JunB in Prostate Cancer"

Verfasserin

Nora Dzuck, Bakk. rer. nat.

angestrebter akademischer Grad

Master of Science (MSc).

Wien, 2012

Studienkennzahl lt. Studienblatt:	A066838
Studienrichtung lt. Studienblatt:	Ernährungswissenschaften
Betreuerin / Betreuer:	Prof. Dr. med. Lukas Kenner

Acknowledgement

I thank Prof. Dontscho Kerjaschki for the possibility to conduct the research for this thesis at the clinical institute of pathology.

I am heartily thankful to my supervisor, Prof. Lukas Kenner, whose encouragement, guidance and support from the initial to the final level of this project enabled me to accomplish this task.

It is a pleasure to thank all of my laboratory colleagues for their help, support, valuable hints and interest namely Susi Heider, Michaela Schlederer, Jan Pencik, Elisabeth Gurnhofer, Tine Vollheim, Astrid Aufinger and Prof. Martin Susani.

I also wish to thank our collaboration group of Zoran Culig at the Medical University of Innsbruck, Stephen Walker and Robert Kennedy for their support.

I would like to give my special thanks to my spouse Felix and my daughter Luna for their encouragement and patient love along the way to complete this thesis.

I also thank my parents and parents in law for consistently supporting me along my studies.

1. Table of Contents

1.1. Table of Figures

1.2.   Table of Tables

1.3. List of Abbreviations

ADT	Androgen deprivation therapy
ALCL	Anaplastic large cell lymphoma
AP	Apical prostate
AP-1	Activator protein-1
AR	Androgen receptor
ARE	Androgen responsive element
BPH	Benign prostatic hyperplasia
BPH-1	Benign prostatic hyperplasia epithelial cell line
BSA	Bovine serum albumin
CDK	Cyclin dependent kinase
CRE	cyclic AMP responsive element
CRPC	Castrate resistant prostate cancer
C_v	Coefficient of variation
CZ	Central Zone
DHT	Dihydrotestosterone
DLP	Dorsal lateral prostate
DRE	Digital rectal examination
DU-145	Androgen independent human prostate cancer cell line
EBRT	External beam radiotherapy
GEM	Genetically engineered mice
GnRH	Gonadotropin-releasing hormone
GS	Gleason Score
GSTP1	Glutathione S-transferase 1
HE	Hematoxylin-Eosin
HGPIN	High grade prostatic intraepithelial neoplasia
HRP	Horse radish peroxidase
HSP	Heat shock protein
IHC	Immunohistochemistry
JNK	cJun N-terminal kinase
LGPIN	Low grade prostatic intraepithelial neoplasia
LH	Luteinizing hormone
LNCaP	Androgen-sensitive human prostate cancer cell line
MAPK	Mitogen activated protein kinase
MEF	Mouse embryonic fibroblasts
PB	Probasin
PBS	Phosphate buffered saline
PCa	Prostate cancer
PCR	Polymerase chain reaction
PC3	Androgen independent human prostate cancer cell line
PDGF	Platelet derived growth factor
PIN	Prostatic intraepithelial neoplasia
PSA	Prostate specific antigen

PTEN	Phosphatase and tensin homolog (gene)
PZ	Peripheral Zone
RARβ2	Retinoic acid receptor β2
Rb	Retinoblastoma protein
RP	Radical prostectomy
RWPF-1	Human prostate epithelial cells
rpm	rounds per minute
SHBG	sex-hormone-binding globuline
SP-1	Specificity protein-1
TAB	Total androgen blockade
TGF-β	Transforming growth Factor-β
TPA	Tumor promoter phorbol-ester
TRE	TPA responsive element
TZ	periurethral transition zone
VCap	Androgen-sensitive human prostate cancer cell line
VP	Ventral Prostate
WB	Western blotting

2. Summary

Prostate cancer is one of the most common cancer types in the Western male population. Yet the underlying mechanisms, which lead to the development of prostate cancer and especially to androgen-insensitivity, are not fully understood. cJun and JunB, two elements of the transcription factor AP-1, have been reported to play a role in various cancer types. They have the ability to act both as tumor suppressor and as oncogene. Their role in prostate cancer is being discussed controversially.

The aim of this thesis is to analyze the effects of cJun and JunB on the development of prostate cancer. Therefore a PB-Cre4 PTEN fl/fl prostate cancer mouse model was used, which included knockouts of cJun and/or JunB. These two proteins were analyzed selectively by means of histologic assessment, immunohistologic experiments and Western blotting.

cJun showed clear tumor suppressing characteristics. Its knockout increased tumor development in prostate cancer mice. Such indicative results could not be attained for JunB, its knockout had neither positive, nor negative effects on tumor development in the prostate.

Our identification of cJun as tumor suppressor in mice prostate cancer correlates with the literature supporting cJun as a tumor suppressor in human. These data should be validated and complemented by data resulting from clinical trials.

3. Zusammenfassung

Prostata-Karzinome gehören zu den häufigsten Krebsarten von Männern in der westlichen Zivilisation. Trotzdem sind die Mechanismen, welche in der Entstehung von Prostata-Krebs und vor allem in der Entwicklung einer Androgen-Insensitivität eine wichtige Rolle spielen, bislang noch nicht vollständig bekannt.

cJun und JunB sind zwei Elemente des Transkriptionsfaktors AP-1, deren Bedeutung schon in verschiedensten Krebsarten nachgewiesen wurde. Sie können sowohl als Tumor-Suppressor als auch als Onkogen wirken. Ihre Rolle im Prostata Krebs wird bis dato kontrovers diskutiert.

Ziel der vorliegenden Arbeit ist es, die Wirkung der beiden Faktoren cJun und JunB auf die Entstehung von Prostata-Karzinomen näher zu untersuchen. Hierfür wurde ein PB-Cre4 PTEN fl/fl Mausmodell verwendet. Dieses Mausmodell beinhaltet neben der Generierung von Prostatakrebs Mäusen auch einen zusätzlichen Knockout von cJun und/oder JunB, um den Einfluss dieser beiden Proteine noch selektiv untersuchen zu können. Eine Analyse der Mäuse wurde mit Hilfe einer histologischen Begutachtung, immunhistologischen Experimenten und Western-Blotting durchgeführt.

cJun zeigte in den Experimenten Tumor supprimierende Eigenschaften. Der knockout von cJun in den Prostatakrebsmäusen verstärkte das Tumorwachstum. Für JunB konnten solche eindeutigen Hinweise nicht gefunden werden. Der knockout von JunB wirkte weder positiv noch negativ auf das Tumorwachstum in der Prostata.

Die starken Hinweise von cJun als Tumorsupressor in Prostata-Krebs Mäusen sind bisher noch nicht beschrieben und unterstützen eher das in der Literatur beschriebene Bild cJun´s als Tumor-Suppressor. Diese Daten sollten weiter validiert und mit humanen Daten komplementiert werden.

4. Aim

The estimated prevalence of cancer cases in 2008 seems to be approximately 12.7 million people worldwide. Prostate cancer (PCa) was, and probably still is, the most common cancer among men in the Western civilization [BRAY et al., 2012].

In 2009,25% of diagnosed malign male tumors in Austria were prostate tumors and PCa was the third most common cancer death in Austrian men [STATISTIK AUSTRIA, 2011].

Recently there has been some progress to resolve the molecular pathogenesis of PCa, however the exact underlying mechanisms are still to be understood. Some of the involved processes are well known while many other factors, which influence the development of PCa, are not yet discovered. Therefore, describing and understanding these factors, plays a major role in developing new treatment strategies in order to treat patients with this condition. The Androgen Receptor (AR) plays a pivotal role in PCa. The aim of a number of studies is to investigate its various functions and how the mechanisms are controlled.

The Activator Protein 1 (AP-1) transcription factor complex can influence the AR in different ways. cJun and JunB are two important members of AP-1. It has been shown that both play a role in the development of tumors. Whether they act as oncogene or as tumor suppressor depends on various factors. The role of cJun in PCa is controversial. As of now, it is unclear whether cJun and JunB act as oncogene or as tumor suppressor in PCa.

Most experiments dealing with PCa were carried out using cell cultures and some were carried out on biopsy specimen of human prostate tissue, like formalin-fixed paraffin embedded tissue (FFPE). FFPE is the standard method to fixate and store tissue samples. In these samples even protein modifications and phosphorylations may be stabilized. With the relatively new reverse phase protein array (RPPA), FFPEs can be analyzed with high throughput and minimal sample wastage [BERG et al., 2010].

To investigate prostate cancerogenesis in greater detail, we took advantage of the Probasin (Pb) Cre4 PTEN$^{loxp/loxp}$ (PTEN$^{pc\ -/-}$) mouse model [KASPER, 2005]. This conditional PTEN knockout model was crossed with various other genetically engineered mice (GEM) to investigate the influence of these genes on the development of PCa.

We were interested in the effect of loss of either cJun or JunB or both alleles on PTEN$^{pc-/-}$ prostate cancerogenesis.

In this thesis the first aim was to crossbreed the PTEN$^{pc-/-}$ prostate cancer mouse model with an additional knockout of cJun and/or JunB to analyze the role of both AP-1 members in PCa. One focus was to investigate the relationship between cJun, JunB and the AR.

5. Introduction

The prostate is an important part of the male reproductive system. The prostate gland is located below the bladder around the urethra. It is composed of fibromuscular stroma and epithelial glands. The stroma consists of smooth muscle cells, fibroblasts, endothelial and dendritic cells, nerves and some infiltrating cells, e.g. lymphocytes and mast cells. The epithelial layer of the glands is built up of basal cells, luminal secretory cells, and endocrine cells. The secretory cells have various important functions, one of which is the secretion of prostate specific antigen (PSA) and some components of the prostatic fluid. They also express the Androgen Receptor (AR). The epithelium of the prostate gland appears to be the origin of the prostate adenocarcinoma [FELDMANN and FELDMANN, 2001].

The stromal-epithelial crosstalk also plays a critical role in the development of PCa. Numerous paracrine factors which are characteristic for the complex interactions of stromal and/or prostate cancer cells have been described, e.g. TGF-β, PDGF, GSTP1 or RARβ2. Angiogenesis, an increase in myofibroblasts and an amplification of the extracellular matrix are characteristic signs of a reactive stroma [NIU and XIA, 2009].

The diagnosis of PCa used to mainly concern elderly men. However, in the last few decades the risk to develop PCa before 75 years of age increased dramatically. In 2009 the risk to develop PCa before the age of 75 was 9% in Austria [STATISTIK AUSTRIA, 2011]. This trend and the increasing life expectancy of males are two of the reasons why an intensified research in the field of PCa is important.

5.1. Screening Test

Localized PCa is hard to detect because in the beginning of PCa very few patients have characteristic symptoms. For this reason screening tests were developed.

A Digital Rectal Examination (DRE) executed by a physician was the primary screening method for a long time. There are two major disadvantages connected to the DRE. The

first issue is that there is a known interobserver bias and secondly, as soon as the prostate is palpable in the DRE, the state of the cancer is usually already advanced [HOFFMANN, 2011].

Today the standard screening method is the measurement of the PSA. This protein is an androgen regulated serine protease and is produced by the prostatic epithelial cells [FREEDLAND, 2011]. PSA can be measured in the blood serum. The normal range is between 0-4 ng/ml and an elevated level of PSA can be associated with PCa. A disadvantage of this screening method is that many results are false positive. This can be due, for example, to benign prostatic hyperplasia (BPH), cystitis, prostatitis, or perianal trauma [HOFFMANN, 2011]. Also a normal level of PSA does not necessarily ensure the absence of PCa.

To confirm the results of DRE and the PSA level a prostate biopsy must be taken. A pathologist histologically examines the prostate tissue for tumor occurrences.

The prostate tissue is graded by the Gleason System according to the 2005 ISUP modification. This grading system assesses 5 different "patterns" ranging from 1, standing for least aggressive tumor, to 5, for most aggressive tumor (Figure 1). The affected prostate often shows different grades of PCa [EPSTEIN et al., 2005].

To determine the Gleason score the two most frequent tumor patterns (grades) are added (for example grade 3+ grade 4 = Gleason Score of 7), which was shown statistically to be of high prognostic value and is guidance for clinical and therapeutic decision [THOMPSON and THRASHER, 2007].
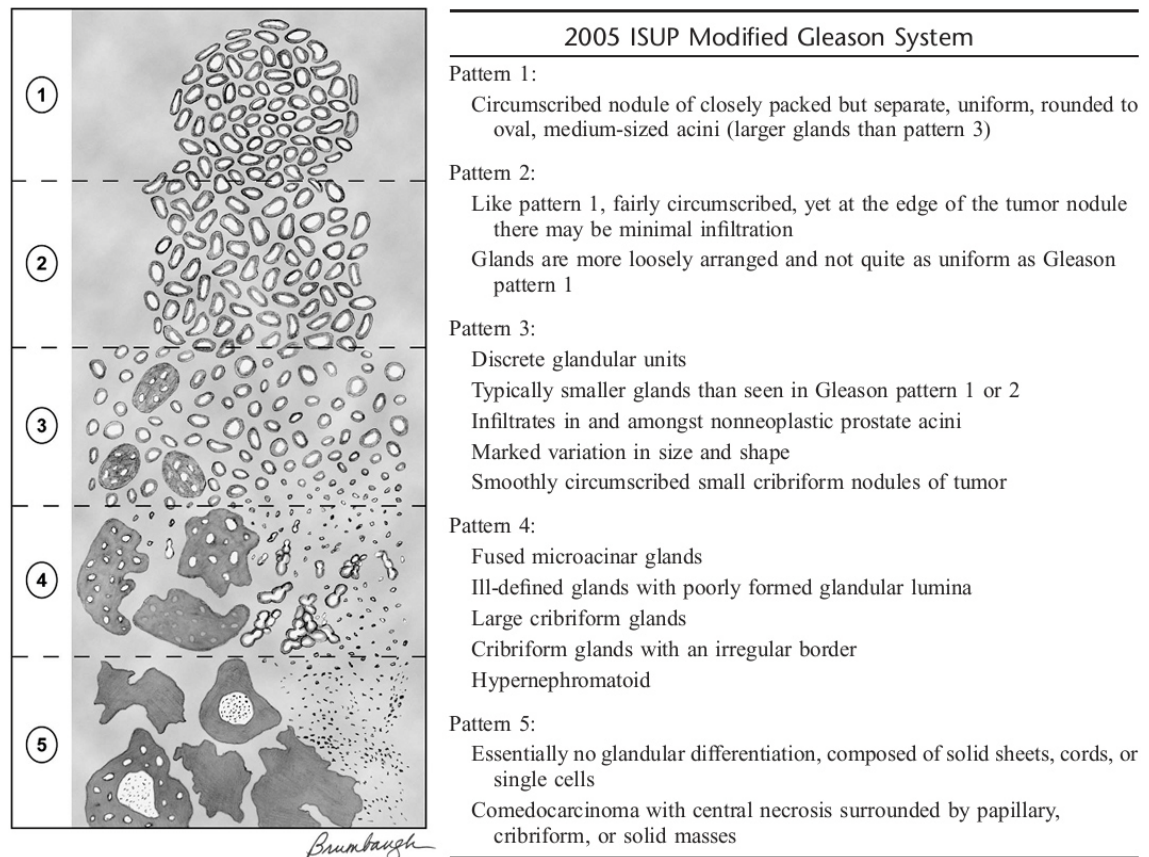
Figure 1: ISUP Modified Gleason System [EPSTEIN et al., 2005].

It is further important to analyze in which degree the tumor has infiltrated the prostate and disseminated into other tissues, e.g. lymph nodes and bone tissue. With this information the tumor can be classified by a staging system, such as TNM classification of the UICC (Greene and Sobin, 2009).The patient risk of disease recurrence or progression can be stratified in low and high risk groups. These stratification schemes involve the PSA level, the Gleason Score, and the tumor staging and are associated with the risk of PSA failure and the various treatment regimens of PCa, e.g. radical prostectomy, chemotherapy or external beam radiotherapy [THOMPSON and THRASHER, 2007]. The risk stratification can be used to choose the treatment according to the risk of relapse [FREEDLAND, 2011].

5.2. Treatment

The optimal strategy for tumor treatment should not only include risk stratification but also life expectancy and the overall health status of the patient [FREEDLAND, 2011].

For low risk prostate cancer patients many treatment opportunities are available and controversially discussed. Some patients undergo an active surveillance with periodic evaluation of the PSA level, DRE, or Gleason score progression on rebiopsy [THOMPSON and THRASHER, 2007]. These patients avoid adverse effects by curative therapies and their risk to die from PCa is low.

Many patients decide for an active treatment of their disease. Most common curative options are radical prostatectomy (RP), external beam radiotherapy (EBRT) and brachytherapy [FREEDLAND, 2011]. Common adverse effects include impotence, and incontinence.

Androgen Deprivation Therapy (ADT) is another treatment option for PCa. If surgical treatment is no option ADT is the mainstay for locally advanced and metastatic PCa. It is also commonly employed in recurrent PCa after RP [YAMAOKA et al., 2010]. In early stage disease ADT is being discussed controversially.

Androgens play an important role in growth and proliferation of the prostate. The testicles produce the majority of the circulating androgens and the minor part is produced by the adrenal gland. Testosterone is the main circulating androgen.
In the blood testosterone is bound to albumin or sex-hormone-binding globulin (SHBG). In the prostate cells it is converted into Dihydrotestosterone (DHT), which has an up to 10 times higher affinity to the Androgen Receptor (AR) than testosterone. Testosterone respectively DHT binds to the AR. The AR is bound to heat shock proteins like HSP 90, 70 or 56. If a ligand like testosterone or DHT binds to the AR-HSP complex, the AR undergoes conformational change and the HSPs dissociate. The AR translocates into the nucleus and dimerizes with another AR molecule. This AR homodimer binds to the androgen-responsive element (ARE) of the target gene. The ARE-bound AR homodimer recruits coactivators or corepressors (which are co-regulators) or interacts

directly with the transcription preinitiation complex of the target gene to either activate or repress these target genes (Figure 2) [HEEMERS H. and TINDALL D., 2007].

AR regulation results in production of PSA, which stimulates growth and survival of cells.

This pathway plays a main role in the development of PCa. Therefore androgens are a main target for treatment of PCa.
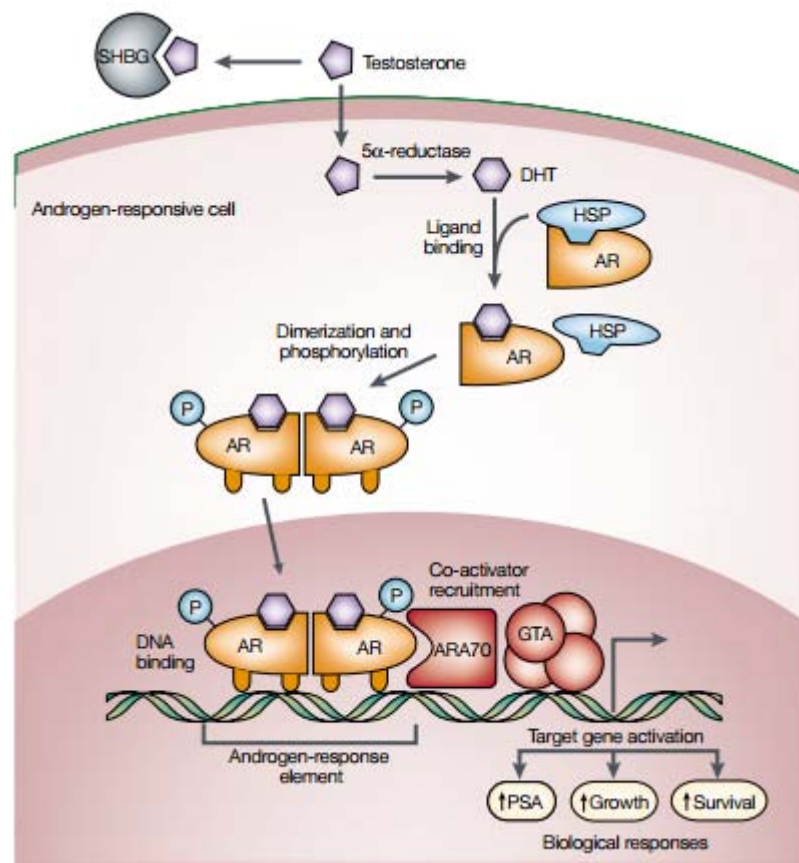
Figure 2: AR interaction: Testosterone enters the androgen-responsive cell. It is then reduced to DHT and binds to the AR within the cytoplasm. HSP meanwhile dislocates from the AR. The AR then dimerizes and binds to the DNA [Feldmann and Feldmann, 2001].

ADT causes androgen ablation, which results in a lower level of PSA and decreased testosterone level [CANNATA et al., 2012].

The first therapeutical approach, ADT, was aiming at the androgen production in the testicles. Orchiectomy and later GnRH agonists are also established methods. Even when serum testosterone is decreased to castrate level prostatic androgen

concentration remains at 10-25 % of the normal androgen level. GnRH agonists prevent the release of Luteinizing Hormone (LH) that is responsible for the androgen production in the testis. Estrogens are no longer used because of their cardiovascular side effects [CANNATA et al., 2012]. The greatest disadvantage of this method is the development of resistance to ADT 2-3 years after start of therapy. This is usually recognized by a newly found increase in PSA in the face of castrate levels of testosterone [FREEDLAND, 2011]. At this point the disease is called castrate resistant prostate cancer (CRPC). Symptomatic CRPC is associated with a poor prognosis [YAMAOKA et al., 2010].

Another important pathway that has a prominent influence on the development of PCa is the PI3K/Akt/mTOR signaling pathway. This pathway is up regulated in 30-50% of PCa. This up regulation is often associated with the loss of the tumor suppressor gene PTEN, which acts as negative regulator of this signaling pathway. Alterations of the PI3K/Akt/mTOR signaling pathway show an increase in tumor grade, tumor stage and risk for recurrence. Many inhibitors for this pathway have been developed. The most promising are mTOR inhibitors [MORGAN et al., 2009].

5.3.   Androgen Receptor and Prostate Cancer

For obvious reasons there is a need to explain the mechanisms underlying CRPC, as well as for solutions to overcome this problem. The exact molecular mechanisms responsible for CRPC are not yet fully understood. Many studies support the importance of the physical presence and the activity of AR [KOOCHEPOUR, 2010].

Androgen Receptor is a nuclear transcription factor which belongs to the steroid-thyroid-retinoid nuclear-receptor superfamily. The biologic activities of androgens are mediated via AR. This is essential for the normal growth of the prostate and for the pathogenesis of PCa [ROSS, 2007].

An altered expression level of AR is one possible mechanism for resistance to ADT. AR amplification leads to enhanced ligand–occupied receptor content even in a low androgen environment [FELDMANN and FELDMANN, 2001].

An increased AR sensitivity is another way to overcome the castrate level of androgens. In CRPC, cells require a four orders of magnitude lower concentration of DHT for growth stimulation as compared to androgen dependent LNCaP cells [FELDMANN and FELDMANN, 2001].

Also the increasing rate of converted testosterone to DHT in prostate cells is a possibility to get over ADT.

All the mechanisms mentioned above should be prevented by an AR-blockade. In total androgen blockade (TAB), one method to inhibit the AR-activity, antiandrogens displace androgens from the AR and block the transcriptional effects of the AR. Drugs like flutamide, nilutamide and bicalutamide are currently used antiandrogens. However, their affinity to the AR is low and all of these antiandrogens eventually fail after a few years of treatment. In these patients the PSA level rises again and the clinical symptoms return [SADAR 2012].

First generation antiandrogens didn't seem to provide any survival benefit. An explanation for this phenomenon could be intratumoral de novo synthesis of androgens. New generations of antiandrogens try to also block these intratumoral androgens [YAMAOKA et al., 2010].

Another alteration that occurs in PCa is AR mutation. In some cases prostate cells with AR mutations can circumvent the growth regulation by androgens. LNCaP cells with a mutation at codon 877 can also be stimulated by nonandrogenic steroids like estrogens or antiandrogens like flutamide. In this case antiandrogens can act adversely as AR activator [KOOCHEPOUR, 2010].

Therefore a new generation of antiandrogens was developed. These new antiandrogens have a higher affinity to the AR and work by different mechanisms than the currently approved antiandrogens e.g. EPI-001. Several small inhibitor molecules have been discovered, for example Pyrvinium pamoate that alters the confirmation of the AR. This small inhibitor protein was tested in a combination with bicalutamide and showed a much higher decrease in prostrate weight than bicalutamide alone [SADAR 2012].

5.4. AP-1

One co-regulator of the AR is the activating-protein 1 (AP-1). In this thesis the relationship between AR and AP1 in prostate cancer shall be investigated.

AP-1 is a dimeric transcription factor that is composed of members of the protein families Jun, Fos, ATF, and MaF. Jun (cJun, JunB, and JunD) and Fos(c-Fos, Fos-B, Fra-1, and Fra2) are the major subfamilies. The AP-1 protein complex can either be homo- or heterodimeric, quite contrary to Fos proteins that cannot homodimerize. The varied combinations of AP-1 proteins determine the regulated genes by affinity and binding specifity. The dimerization of AP-1 is promoted by a leucine zipper motif and has a basic domain to interact with the DNA. [EFERL and WAGNER, 2003]

It recognizes the TPA responsive element (TRE) and the cyclic AMP responsive element (CRE). Positive or negative regulation of target genes of AP-1 depends on dimerization composition, the abundance of dimerization partners, posttranslational modifications and also the interaction with other proteins [VESELY et al., 2009].

5.5. cJun and JunB

In this thesis the focus lies on cJun and JunB, two members of the Jun subfamily. They are well investigated and show high potential in the regulation of tumorigenesis.

Translational control mechanisms can control the abundance of AP-1 proteins. The translation of JunB is regulated by mTOR. The control mechanisms for the mRNA of cJun are CAP-dependent or CAP-independent and regulated via IRES, the internal ribosome entry segments [VESELY et al., 2009].

Posttranslational modifications play an important role in the activity and binding specificity of cJun and JunB. The principal activation of cJun and JunB occurs via phosphorylation. In general extracellular signals are mediated through protein kinase cascades that lead to phosphorylation of the specific transcription factor.

Detailed information on the regulation of phosphorylation of cJun exists and is described below. JunB phosphorylation mechanisms have hardly been investigated [PIECHACZYK and FARRAS, 2008].
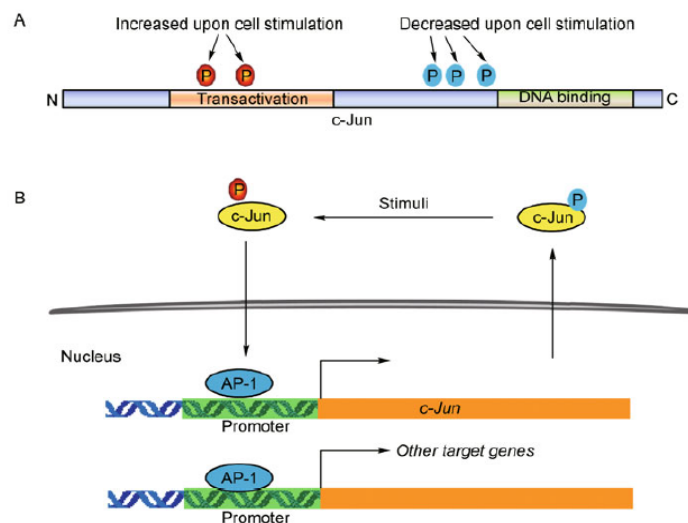
Figure 3: Feed-forward regulation and expression of cJun. Intracellular cJun-phosphorylation of the transactivation region leads to AP-1-activation which in turn leads to increased cJun expression [MENG and XIA, 2011].

cJun has five serine and threonine residues where phosphorylation can take place. Upstream the DNA-binding site three phosphorylation sites exist and two sites are located in the N-terminus (Figure 3) [MENG and XIA, 2011].

There is a feed forward mechanism between AP-1 and cJun expression. AP-1 stimulates the cJun promoter and gene expression. Upon expression cJun in turn increases AP-1 and thereby potentiates the cJun promoter activation. Through this autocrine amplification loop cJun is able to convert transient biochemical signals to long running AP-1 activity [MENG and XIA, 2011].

Phosphorylation of cJun takes place via the mitogen activated protein kinase (MAPK) cascade. MAP-3K is induced by physiological and environmental factors like mitogens and stress (TNF, UV light). It catalyzes MAP-2K (MEK 1-4, 6 and 7) by phosphorylation. MAP-2K in turn activates MAPK. Three groups of MAPK exist: JNK, ERK, and p38. For the regulation of cJun phosphorylation of JNK and ERK is essential (Figure 4) [MENG and XIA, 2011].
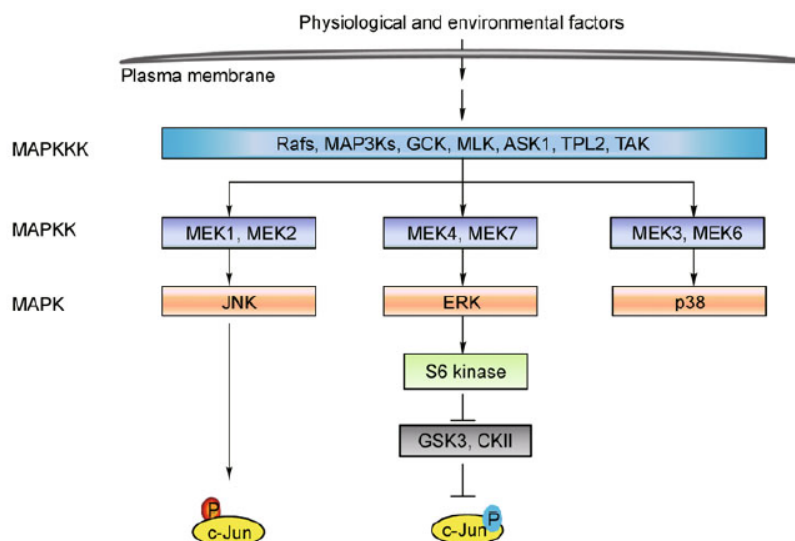
Figure 4: Signaling pathways leading to cJun phosphorylation [MENG and XIA, 2011]

GSK-3 and CKII can phosphorylate cJun at the c-terminal domain. Thereafter, cJun is in a non-binding state. ERK can activate the S6 kinase that in turn inactivates GSK-3. An increased level of ERK leads to dephosphorylation of cJun in the C-termini and therefore enhances the binding activity to the DNA. JNK can bind to the transactivation domain of cJun and phosphorylates cJun at the N-termini [MENG and XIA, 2011].

DNA binding and transcription of cJun can be enhanced by the tumor promoter phorbol-ester (TPA). It decreases the phosphorylation in the C-termini and thereby increases the DNA-binding of cJun. Furthermore, TPA induces the transactivation activity of cJun by increasing the N-terminal phosphorylation [MENG and XIA, 2011].

As mentioned before there is no detailed information on JunB phosphorylation, but it is known that the phosphorylation sites at serine 63 and 73 for JNK are not conserved in JunB [PIECHACZYK and FARRAS, 2008]. On the other hand Li et al discovered a phosphorylation of JunB by JNK at threonine 102 and 104. Thus phosphorylated JunB stimulates IL-4 expression in T-helper cells [LI et al 1999].

The influence of cJun and JunB on the cell cycle partly explains their role in tumorigenesis. They regulate various genes that significantly affect the cell cycle and apoptosis (Table 1**).**

Gene product	Activity	cJun	JunB
Cyclin D1	Proliferation ↑	Up	Down
p53	Proliferation ↓ Apoptosis ↑	Down	-
p21^{Cip1}	Proliferation ↓	Down	-
p16^{INK4}	Proliferation ↓ Apoptosis ↑	Down	Up
p19^{ARF}	Proliferation ↓ Apoptosis ↑	-	-
GM-CSF	Proliferation ↑	Up	Down
KGF	Proliferation ↑	Up	Down
HB-EGF	Proliferation ↑	Up	-
FL1	Proliferation ↑	Up	Up
FasL	Apoptosis ↑	Up	-
Fas	Apoptosis ↑	Down	-
Bcl3	Apoptosis ↓	Up	-

Table 1: AP-1-regulated genes, that significantly affect cell cycle progression and apoptosis [SHAULIAN and KARIN, 2002].

In quiescent cells expression of cJun and JunB is low. They reach their expression peak during G_0/G_1 transition and return to an intermediate level. For cell cycle progression towards S phase this induction is instrumental. The high expression of cJun in G_1 results from N-terminal phosphorylation. During the rest of the cell cycle cJun levels remain constant. JunB levels increase in G_1 phase and on entering S phase. In G_2/M phase the level of JunB is low (Figure 5) [PIECHACZYK and FARRAS, 2008].
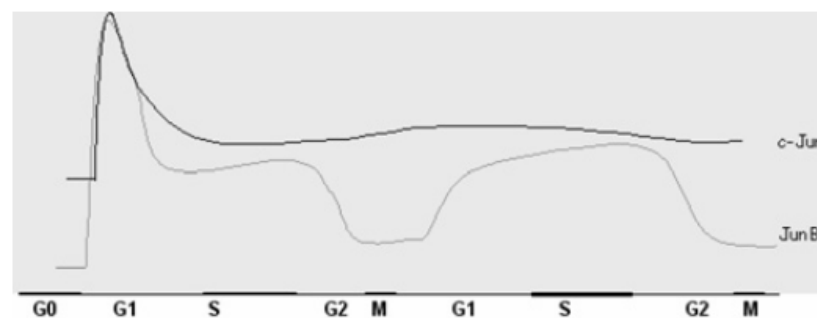
Figure 5: cJun and JunB levels during the cell cycle. Both, cJun and JunB levels, peak just after the cell leaving G0 phase, cJun then retains quite constant concentration whereas JunB levels drop dramatically when entering the M phase, then returns to normal levels again in G1 phase [PIECHACZYK and FARRAS, 2008].

cJun induces the transcription of cyclin D1. Furthermore, cJun directly represses p53 gene transcription. cJun also has the ability to decrease the transcriptional activity of the tumor suppressor p53. It reduces the ability of p53 to activate the p21 gene. P21

inhibits the cyclin dependent kinase (CDK) [SHAULIAN and KARIN, 2002]. Taken together cJun positively regulates the cell cycle through the induction of cyclin D1 transcription and the repression of p21 transcription (Figure 6).

All these effects of cJun boost proliferation and in case of proliferation are associated with cancerogenesis. In diseases like Anaplastic Large Cell Lymphoma (ALCL) and Hodgkin´s disease cJun is overexpressed. It suppresses the apoptosis in ALCL cells and increases proliferation in Hodgkin's disease [SHAULIAN, 2010].

On the other hand cJun can also act proapoptotic and antiproliferative. It induces apoptosis following adequate DNA damage after exposing cells to UV light. cJun is also involved in DNA repair mechanisms. cJun-deficient MEF`s (mouse embryonic fibroblasts) show an impaired repair mechanism and strongly damaged DNA. It depends on the extent of damage by UV-radiation whether cJun promotes DNA-repair and cell cycle reentry or apoptosis. [SHAULIAN, 2010].

cJun can also regulate proapoptotic genes like Fas, FasL, Bim and antiapoptotic genes like Bcl_3. The balance of expression of such genes regulates whether the cells survive or undergo apoptosis (Figure 6) [SHAULIAN and KARIN, 2002].
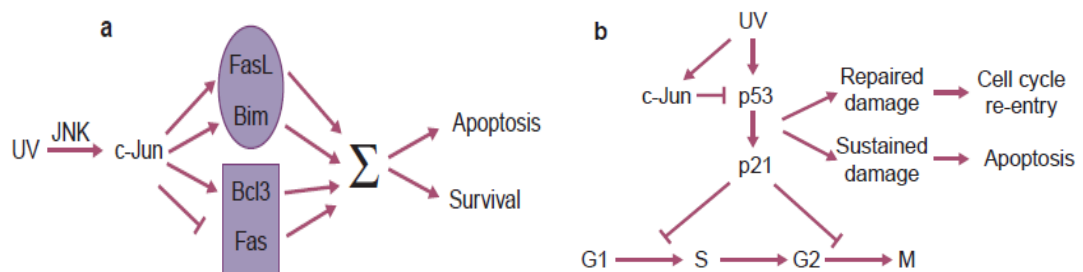
Figure 6: Effects of cJun in apoptosis. a) Upon UV-exposure of cells showed that cJun mediates induction of pro-apoptotic genes (FasL, Bim) as well as up-regulation of anti-apoptotic genes (Bcl3) and downregulation of pro-apoptotic gene products (Fas). The sum of these regulations leads to the cell undergoing apoptosis or survival respectively. b) cJun leads to downregulation of p21, which is, on the whole, an anti-apoptotic action. Yet cells exposed to UV will still undergo apoptosis, if cell damage is sufficient [SHAULIAN and KARIN, 2002].

Both cJun and JunB expression elevates the level of Dmp1. This tumor suppressor enhances the expression of p19[ARF], another tumor suppressor that increases p53 activity. This is due to interaction with Mdm2 [SHAULIAN and KARIN, 2002].

In summary the function of cJun is controversial and depends on many factors.

Like cJun, JunB can also act as a tumor suppressor and, in a different setting, as oncogene.

In ALCL JunB expression is increased and enhances proliferation. This is due to the fusion protein npm-alk (anaplastic lymphoma kinase). This oncogenic protein increases JunB levels via the mTOR pathway [SHAULIAN, 2010].

The function of JunB in the cell cycle is the repression of the promoter of cyclin D1 and the induction of p16. Overexpression of JunB leads to an upregulation of p16 and thereby inhibits phosphorylation of Rb by CDKs. This prevents the transition from G_1 to S-phase. Overexpression of JunB also inhibits the induction of cyclin D1 by cJun. JunB acts antiproliferative and antagonizes cJun, but it also has promoting activities in the cell cycle. JunB is needed for a rapid progression during S-phase. It positively regulates the transcription of cyclin A_2 [SHAULIAN and KARIN, 2002].

Before mitosis JunB degrades depending on phosphorylation. The decreased JunB levels during mitosis ensure an adequate progression into the next G_1-phase (Figure 7) [PIECHACZYK and FARRAS, 2008].

To sum up the effects of JunB it can inhibit the cell cycle by antagonizing cJun, repressing cyclin D1 and inducing p16. On the other hand JunB is important for cellular proliferation in ALCL and can promote the cell cycle through induction of cyclin A_2.
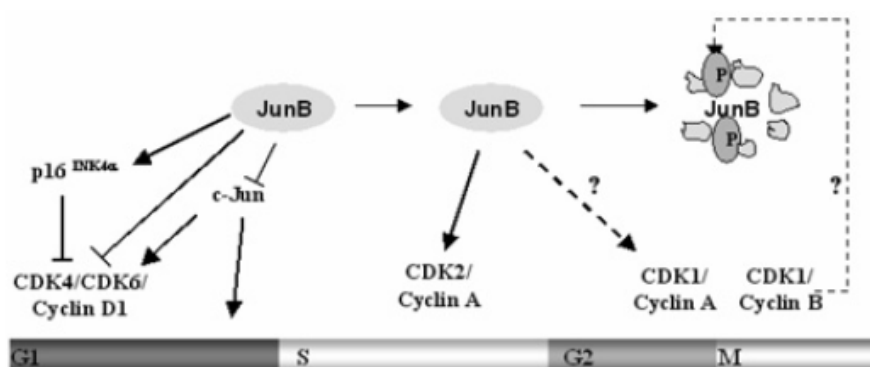
Figure 7: Cell cycle-inhibiting and -promoting activities of JunB. JunB mediates up-regulation of p16 and inhibits cJun, thereby inhibiting the cell cycle. It also induces Cyclin A2, thereby driving the cell cycle. The overall effect depends on the sum of interactions [PIECHACZYK and FARRAS, 2008].

The effects of cJun and JunB greatly depend on the circumstances. The question remains, how their expression impacts PCa and its development.

5.6.   cJun and JunB and AR

The expression levels of cJun in the prostate and therefore its relevance to prostate tissue is being discussed controversially. In a study of Ricote et al p-cJun levels in normal prostate, benign prostate hyperplasia (BPH) and PCa were observed via immunohistochemistry and Western Blotting (WB). In both experiments the normal prostate tissue and PCa samples showed no expression of p-cJun. Interestingly in 27% of BPH samples p-cJun expression was observed [RICOTE et al., 2003].

On the other hand a study of Tiniakos et al showed cJun expression in 13 of 16 (81.25%) patients with BPH. In PCa 31 of 36 (86.1%) patients showed cJun expression. Additionally, they found no correlation between the expression of cJun and PSA-level or Gleason score [TINIAKOS, 2006].

Many studies tried to investigate the various mechanisms in which cJun is involved in PCa or influences the AR. It has been shown that cJun functions as coactivator of AR that stimulates the transactivation of AR. This occurs via mediation of receptor dimerization and a subsequent binding to DNA [CHEN et al., 2006].

Furthermore in LNCaP cells a direct correlation between endogenous level of cJun and the activity of AR transcription and also with the androgen regulated genes was observed. The function of cJun as AR-coactivator in LNCaP cells seems to be more sufficient for the regulation of androgen dependent growth than AP-1 transactivation. This was tested in a cJun mutant LNCaP cell line that is less active in AP-1 transactivation and fully active in AR-coactivation. The results show an increase of proliferation in androgen dependent LNCaP cells [CHEN et al., 2006].

cJun is also involved in protein-protein interactions that can influence the AR function. If cJun, Sp1, and AR form a protein complex induced by the plant-polyphenol Quercitin, the function of AR appears to be suppressed in PCa cells. This complex inhibits the positive effect of Sp1 on AR transcriptional activity by the transcriptional function of AR to regulate androgen dependent genes [YUAN et al., 2010].

On the whole, it has been shown that the impact of cJun in PCa is multifactorial and that it is being discussed controversially.

Studies concerning the influence of JunB on PCa are rare. Some few studies have analyzed the JunB expression profile in PCa but none have investigated the relationship of JunB and the AR.

An extensive study of expression profiles in PCa also examined JunB expression. They investigated donor-, primary and metastatic PCa. High expression of JunB was observed in primary prostate samples. In donor and metastatic tumors a low JunB expression was detected (Figure 8) [CHANDRAN et al., 2007].
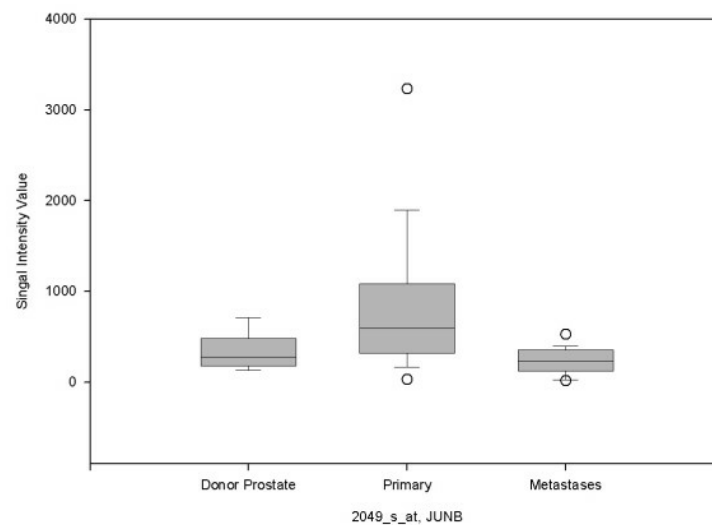
Figure 8: JunB expression of donor prostate samples, primary and metastatic PCa. In primary PCa JunB seems to be up-regulated [CHANDRAN et al., 2007].

In another study an inverse correlation between JunB expression and an increase of the pathological grade in primary and metastatic human PCa was detected. JunB expression was examined immunohistologically. In normal prostate epithelium the expression of JunB is 61.7± 3.45%. The higher the Gleason grade, the lower was the JunB expression (GS<6 43.3± 4.44% and GS=8 11.6 ±1.94%). In metastasis just 1.93± 0.26% JunB expression was observed (Figure 9) [KONISHI et al., 2008]. Based on this study JunB could have tumor suppressor activities.
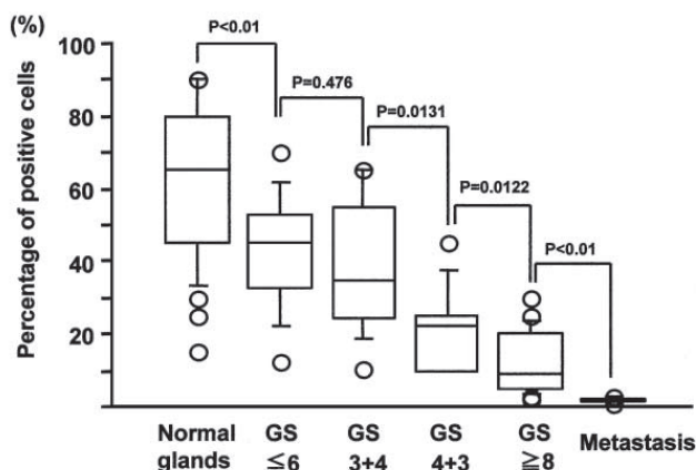
Figure 9: JunB expression in primary and metastatic PCa. With increasing Gleason Score JunB levels decrease significantly [KONISHI et al., 2008].

Further research work directly concerning cJun, JunB and AR was done by Puhr et al. unpublished. Six prostate cell lines were analyzed for their expression of AR, cJun, and JunB using Western Blotting. Two wildtype prostate cell lines (RWPF-1 and BPH-1), two androgen dependent (VCaP and LNCaP), and two androgen independent (DU145 and PC3) prostate cancer cell lines were investigated (Figure 10).

In the wildtype and the androgen independent prostate cell lines the AR was rarely expressed. However, in the androgen dependent prostate cell lines the AR was highly expressed. cJun and JunB act exactly in the opposite way. In RWPF-1, BPH-1, and in DU145, PC3 cJun and JunB were highly expressed. In contrast the VCaP and LNCaP cells did not express both AP-1 proteins. In prostate cell lines AR, cJun, and JunB seem to directly influence each other [PUHR et al., unpublished).

Taking together, the results are controversial. AP-1 components may have many different effects in PCa. Some mechanisms are fully understood but many still remain unclear.

The influence of cJun and JunB in prostate cancer mouse models is barely studied. They are, however, very promising targets in PCa development, even though the existing data are rather controversial, possibly due to the complexity of the involved mechanisms. Since it is known, that the AR plays an important role in PCa genesis the

aim of thesis at hand will be to take the current research to the next level and study the effects of a cJun and/or JunB knockout on the AR in mice.
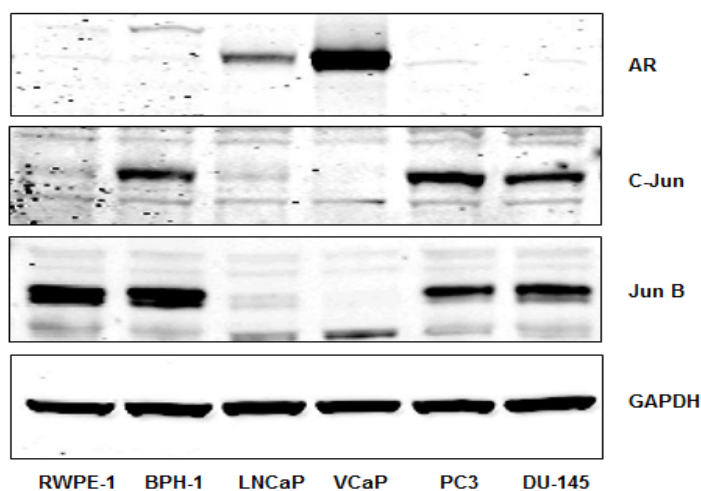
Figure 10: Protein expression of AR, cJun and JunB in wt, androgen dependent and androgen independent prostate cancer cell lines. No elevated AR expression is seen in the wt prostate cells (RWPE-1, BPH-1), yet cJun and JunB expression is up-regulated. In the androgen dependent prostate cancer cell lines (LNCaP, VCaP) the AR expression is increased, whereas cJun and JunB expression is decreased. In the androgen-independent prostate cancer cell lines (PC3, DU-145) the AR expression is decreased and cJun and JunB expression is increased again [PUHR et al., unpublished data].

In mouse and human prostates many anatomical similarities exist that make it possible to take GEM for investigating human diseases like PCa.

Both species have a male accessory organ that develops from the urogenital sinuses and the Wolffian ducts. Their prostates form lobular glands and are androgen specific. Both have differentiated prostate epithelial cells and their function is similar [SHAPPELL et al., 2004].

Obviously, there are also anatomical differences between mouse and human prostates which have influence on the pathological interpretation of the mouse model.

In the adult human organism the prostate is no longer clearly separated into lobular structures, as it is in mice. It is rather divided into different zones: periurethral transition zone (TZ), peripheral zone (PZ), and central zone (CZ). BPH is often formed in the TZ and PZ is often the origin of PCa. CZ is seldom the origin of PCa (Figure 11) [SHAPPELL et al., 2004].
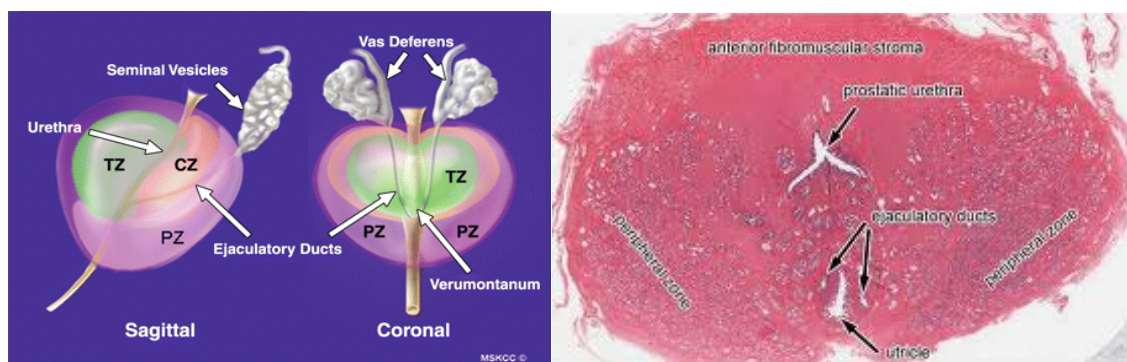
Figure 11: a) Schematic anatomy of zones of the prostate gland. CZ = central zone; TZ = periurethral transition zone; PZ = peripheral zone [CURRAN et al., 2007]. b) HE prostate gland [http://www.med.umich.edu/histology/endoRepro/questions/slide281orientation.jpg].

As mentioned before the mouse prostate is composed of distinct lobes: Apical Prostate (AP), Ventral Prostate (VP), and Dorsal and Lateral Prostate (DLP)). The lobes are surrounded by a capsule lined with mesothel (Figure 12) [SHAPPELL et al., 2004]. For investigation of PCa all different mouse prostate lobes are equally relevant. In each mouse prostate gland cell populations are normal and homologous to the human prostate. There is a basal cell layer, luminal secretory cells and some neuroendocrine cells [SHAPPELL et al., 2004].
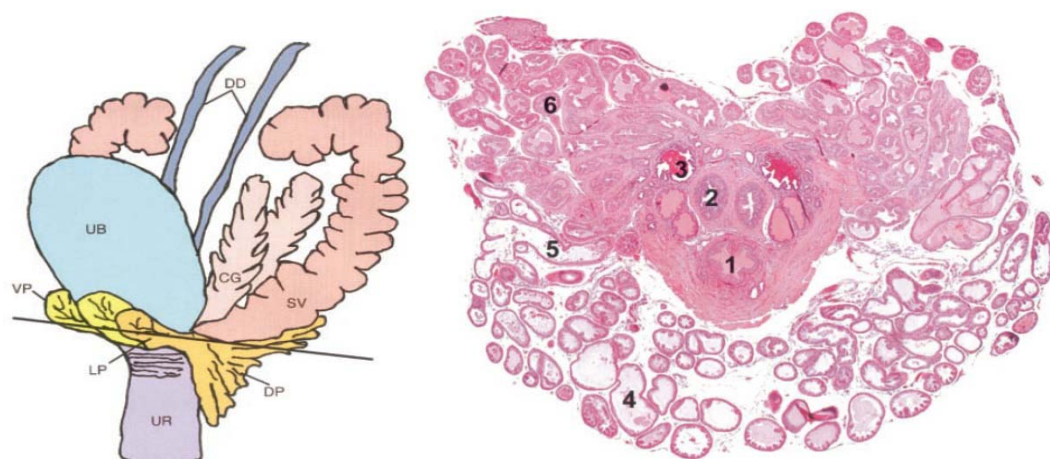
Figure 12: a) Schematic diagram of the mouse genitourinary bloc. UB = urinary bladder; VP = ventral prostate; LP = lateral prostate; DP = dorsal prostate; SV = seminal vesicals; CG = coagulating gland or anterior prostate; DD = ductus deferens; UR = urethra. b) Microscopic section of the mouse prostate gland. 1 = urethra; 2 = ductus deferens; 3 = ampullary glands; 4 = venral prostate; 5 = lateral prostate; 6 = dorsal prostate [SHAPPELL et al., 2004].

PCa does not develop spontaneously in mice [SHAPPELL et al., 2004]. For research in the field of PCa in mice some genetically engineered mice (GEM) were created.

Traditional gene targeting has some limitations and did not result in good PCa models. In conventional knockout mice the timing of gene disruption is not under the researcher's control. However, this is pivotal in a PTEN PCa model because the knockout of PTEN during embryogenesis is lethal. Aside from the timing it is better that the gene disruption occurs only in specific celltypes or tissues. Both these requirements are met using a conditional knockout strategy [STRICKLETT et al., 1999].

The Probasin Cre4 PTEN$^{loxp/lox}$ system is a frequently used model to simulate PCa in mice. With this PTEN model the development, the tumor progression and metastasis of PCa can be observed [KASPER, 2005].

The Cre loxP recombination system is conditional, cell type-, and tissue-specific. The limitation of this method is the availability of a specific promoter. Cre is a site specific DNA recombinase. Between loxP sites Cre excises DNA sequences [WU et al., 2001]. To drive Cre expression in the prostate the Probasin promoter seems to be a good choice. Probasin expression is regulated by androgens and primarily observed in differentiated secretory epithelial cells [JOHNSON et al., 2000].
Expressed with the Probasin promoter Cre activity was observed in luminal epithelium of the prostate lobes but not in basal cells. In prostatic buds of newborns the Cre activity was low but an increasing Cre expression was detected until adulthood [WU et al., 2001].

The deletion of PTEN in the prostate is very critical for tumor development. PTEN is a tumor suppressor located on chromosome 10. The loss of PTEN is frequently mapped in primary human PCa. It is a lipid phosphatase and dephosphorylates products (3-phosphoinosites) of the PI3K-pathway. 3-phosphoinosites can activate survival kinases such as Akt. The Akt pathway controls cell cycle progression, cell proliferation and the escape from apoptosis via MDM2, p21, p27, Caspase9, GSK3 and others. PTEN negatively regulates the Akt-pathway [HOLLANDER et al., 2011].

Taken together, to create a PCa mouse model such as PB Cre4 PTEN$^{loxP/loxP}$ loxP sites to the flanking regions of the PTEN gene have to be inserted. In another mouse the transgene Cre had to be inserted into the Probasin promoter region. Breeding the

PTEN$^{loxP/loxP}$ mouse with the PB Cre mouse leads to excision of PTEN in prostate epithelial cells (PTEN$^{pc-/-}$). In all other cell types and tissues of the mouse PTEN remains still active (Figure 13).
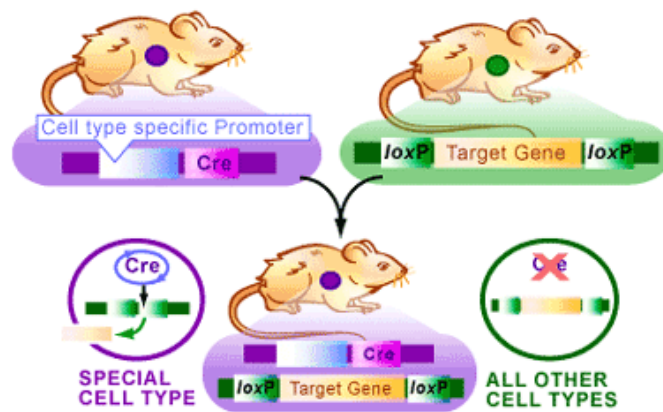
Figure 13: Cre/lox System. Cre+ mouse crossed with a mouse with a target gene with loxP sites leads to excision of target gene in the offspring [PECHIKSER, 2004].

If one allele of PTEN is knocked out (PTEN$^{pc+/-}$) the mice develop tumors in the prostate from nine month of age. A complete deletion of PTEN leads to PIN lesions at the age of six weeks. An invasive and metastatic PCa was observed within a few weeks. Mice of this PTEN model are responsive to androgen ablation that prolonged survival. In mice with this ADT highly proliferating tumors were found in necropsy. It seems that in this model CRPC (castrate resistant prostate cancer) can arise in the mice after ADT [HOLLANDER et al., 2011].

For the reasoning above the described mouse model was used to conduct the research on the thesis at hand.

6. Methods

6.1. Mouse Breeding

Male mice with the genotype Cre+ PTEN fl/fl were used for the experiments. To achieve this genotype male Cre+ mice were crossed with female PTEN fl/fl mice in a first breeding (figure14). In a second breeding step Cre+ PTEN fl/+ male mice were crossed with female Cre- PTEN fl/+ mice to come by the desired genotype, male Cre+ PTEN fl/fl.
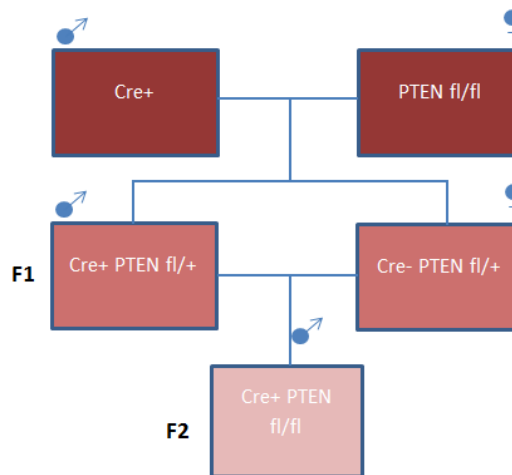
Figure 14: Breeding scheme of the first breeding.

The resulting genotypes were used to validate the outcome. With HE-stainings mice prostates (wildtype, Cre+ PTEN fl/+ and Cre+ PTEN fl/fl, or wildtype, PTEN$^{pc+/-}$, PTEN$^{pcfl/fl}$ respectively) were analyzed to occurrence and severity of prostate cancer, respectively. These three genotypes were also used to interpret the influence of cJun and JunB in the PTEN knock out mouse model.

In the second breeding step AP1-proteins (floxed alleles of JunB and cJun) were bred in. Female Cre+ PTEN fl/fl mice were crossed with male cJun fl/fl and JunB fl/fl mice. From the first generation (F1) male Cre+ PTEN fl/+ cJun fl/+ JunB fl/+ and female Cre- PTEN fl/+ cJun fl/+ JunB fl/+ were crossed with each other to generate the final genotypes (F2: Cre+ PTEN fl/fl with cJun fl/fl JunB fl/fl and Cre+ PTEN fl/fl cJun fl/fl

JunB +/+ and Cre+ PTEN fl/fl cJun +/+ JunB fl/fl, or PTEN$^{pc-/-}$ cJun$^{pc-/-}$ JunB$^{pc-/-}$, PTEN$^{pc-/-}$ cJun$^{pc-/-}$ JunB$^{pc+/+}$ and PTEN$^{pc-/-}$ cJun$^{pc+/+}$ JunB$^{pc-/-}$ respectively) (Figure 15).

To better understand the role of cJun and JunB, heterogeneous knock outs of JunB and cJun were also analyzed (F2: Cre+ PTEN fl/fl cJun fl/+ JunB fl/+ and Cre+ PTEN fl/fl cJun fl/+ JunB +/+, Cre+ PTEN fl/fl cJun +/+ JunB fl/+, or PTEN$^{pc-/-}$ cJun$^{pc+/-}$ JunB$^{pc+/-}$ and PTEN$^{pc-/-}$ cJun$^{pc+/-}$ JunB$^{pc+/+}$, PTEN$^{pc-/-}$ cJun$^{pc+/+}$ JunB$^{pc+/-}$ respectively) (Figure 15).

The final outcome of the breedings was comprised of 6 genotypes that were analyzed by immunohistochemistry and western blotting. All mouse experiments were carried out in accordance to the Austrian Act on Animal Experimentation (GZ 66.009/139-II/106/2009).
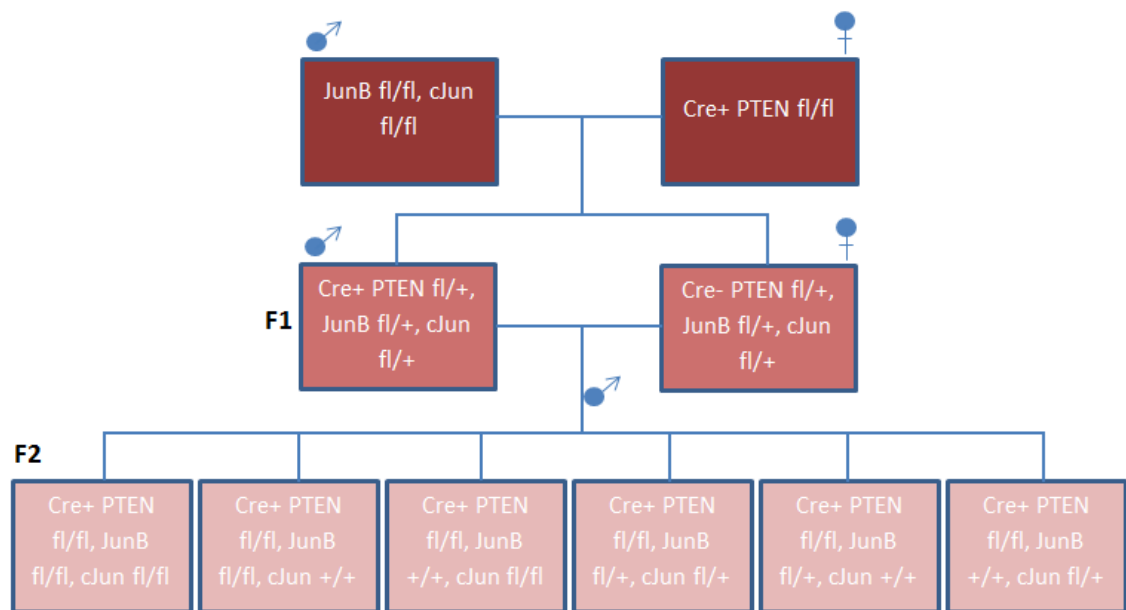
Figure 15: Breeding scheme of the second breeding.

6.1.1. DNA Isolation

At the time of determination of the genotype the mice were between three and four weeks old. 0.5 cm of the mouse tail was cut off and 400 µl DNA extraction buffer and 20 µl of proteinase K (10 mg/ml) was added. The tail was incubated over night at 55 °C while shaking. The lysed tissue was mixed for 5 min using an Eppendorf mixer. For the precipitation of DNA 200 µl NaCl (5M) was added and mixed for an extra 5 min on an

Eppendorf mixer. After centrifugation for 10 min at 13000 rpm (15682 x g) (Eppendorf 5415D) 530 µl were taken from the upper phase and transferred into a new 1.5 ml tube. 400 µl isopropanol was added, mixed for 2 min and centrifuged at 13000 rpm for 5 min. The pellet was washed with 1 ml ethanol (70 %) and centrifuged again a 13000 rpm (15682 x g) for 5 min. The supernatant was discarded and the pellet resuspended in 200 µl aqua dest. The DNA solution was incubated at 37 °C for 2 h while shaking. After this procedure the DNA solution was used for PCR or, alternatively, stored at 4 °C.

DNA Extraction buffer:

50 mM   Tris pH 8
100 mM   EDTA pH8
100 mM   NaCl
1 %   SDS
filled up to 50 ml with aqua dest.

6.1.2. DNA Amplification with PCR

The concentration of the resulting mouse DNA was not high enough for further analysis. Using Polymerase chain reaction (PCR) it is possible to create and amplify the DNA sequence of interest using specific oligonucleotid primer pairs.

Used Primers:

	Sense	antisense
PTEN wt, fl	5'-CTCCTCTACTCCATTCTTCCC-3'	5'-ACTCCCACCAATGAACAAAC-3'
PTEN Δ	5'-GTCACCAGGATGCTTCTGAC-3'	5'-ACTATTGAACAGAATCAACCC-3'
JunB wt, fl	5'-GGGAACTGAGGGAAGCCACGCCGAGAAAGC-3'	5'-AGAGTCGTCGTGATAGAAAGGC-3'
JunB Δ	5'-GGGAACTGAGGGAAGCCACGCCGAGAAAGC-3'	5'-AAACATACAAAATACGCTGG-3'
cJun wt, fl	5'-CTCATACCAGTTCGCACAGGCGGC-3'	5'-CCGCTAGCACTCACGTTGGTAGGC-3'
cJun Δ	5'-CTCATACCAGTTCGCACAGGCGGC-3'	5'-CAGGGCGTTGTGTCACTGAGCT-3'
Cre	5'-CGGTCGATGCAACGAGTGATGAGG-3'	5'-CCAGAGACGGAAATCCATCGCTCG-3'

Table 2: Used sense and antisense primer for PCR for each analyzed gene.

PCR consists of multiple cycles of varying temperature steps. The cycles are repeated several times (see PCR Program below). The first step is the denaturation. Hydrogen bonds between complementary bands are disrupted at 90-94 °C resulting in single stranded DNA-Templates. The next step is Annealing, in which the primers hybridize

with the complementary DNA strands at ≥ 50 °C. The Taq-polymerase synthesizes the sequence of interest at 72 °C which is the last step called Elongation. After each cycle the DNA amount is doubled. This leads to exponential amplification of the DNA template. For the different DNA templates the PCR program has to be adjusted frequently resulting in varying PCR programs.

Set up PCR reaction reagents	PCR Program Cre, JunB, cJun, cJunΔ	PCR Program JunB Δ, PTEN, PTEN Δ
12 µl GoTAQ Green MM	5 min at 95 °C	5min at 95 °C
0.5 µl DMSO	30 sec at 95 °C ⎤	30sec at 95 °C ⎤
0.5 µl primer forward	30 sec at 58°C ⎬ 32x	30sec at 55 °C ⎬ 32x
0.5 µl primer reverse	1 min at 72 °C ⎦	1min at 72 °C ⎦
0.5 µl aqua dest.	10 min at 72 °C	10min at 72 °C

6.1.3. Gel electrophoresis

For analyzing the DNA, the samples were examined using gel electrophoresis. With this method DNA fragments are separated by their size. The DNA samples were applied on a 2 % agarose gel supplemented with Midori Green (1 µl/100 ml gel). Midori Green intercalates with the DNA and absorbs UV light. After gel electrophoresis with 120 V for about 15 min the DNA bands were visible under UV light and were analyzed. Some primer pairs have two DNA products. The first one is the wt DNA product of the target gene and the second is the floxed DNA fragment of the target gene. This is the case for JunB, cJun and PTEN. If there are two bands the mouse has one wt allele and one floxed allele. If there is just one band the mouse has either wt or floxed alleles, which can be differentiated by their molecular weight.

<u>2 % Agarose gel:</u>

2 g Agarose
100 ml TAE buffer

<u>TAE buffer:</u>

96.8 g TRIS
22.8 ml glacial acetic acid
40 ml 500 mM EDTA
filled up to 20 l with aqua dest.

PTEN wt	209	JunB Δ	320
PTEN fl	335	cJun wt	280
PTEN Δ	849	cJun fl	320
JunB wt	300	cJun Δ	600
JunB fl	350	Cre	455

Table 3: PCR products in bp.

6.2. Prostate Sample Preparation

After 19 weeks male mice were sacrificed. The genito-urinary tract with the prostate, seminal vesicals, and the bladder was resected and weighed. Thereafter a macroscopic picture was taken. The next step was the isolation of the prostate. Care was taken to remove as much fat tissue as possible from around the prostate and to avoid inclusion of pieces of the bladder or the seminal vesicles into the prostate sample. The whole prostate was weighed and then cut up into two pieces.

One piece was fixed with 4.5 % paraformaldehyde. After dehydration the sample was embedded in paraffin and stored at room temperature. The other piece of the prostate was first put into liquid nitrogen and later stored at -80 °C.
The documented body- and prostate weight of the mice was analyzed statistically. First the means ($\bar{x}$) of the body- and prostate weight in each genotype were determined and thereafter the standard deviation (s). To relativize the standard deviation and to check whether the means were representative for all data the coefficient of variation (C_v) was calculated.

$$\bar{x} = \frac{x1 + x2 + \cdots + xn}{n} \qquad S = \sqrt{S^2} := \sqrt{\frac{1}{n-1} \sum_{i=1}^{n} (X_i - \bar{X})^2} \qquad c_v = 100 \frac{s}{\bar{x}}$$

Furthermore, the results of the genotypes in the bodyweight- and prostate weight groups were analyzed by an unpaired T-Test. This Test compares whether the differences of two independent groups of samples are statistically significant. This is expressed by the p-value.

6.3. Hematoxylin-Eosin (HE) Staining

For histochemical staining (HE-staining and IHC immunohistochemistry) 3 µm sections were cut off the paraffin block with the prostate sample. The prostate sections were placed on microscope slides.

To evaluate the prostate tissues with different genotypes HE staining was done. This is a standard procedure to initially screen whether the tissue samples are regularly aligned or irregular as seen, for example, in cancer. After the staining procedure the cell nucleus will be colored blue (hemalaun) and the cell plasma will be colored red (Eosin).

The tissue slides were placed in a staining machine (Tissue Stainer COT20, Medite GmbH Germany). The progression in the staining program was as follows and done automatically. In a first step the tissue samples were deparaffinized. The next step was the incubation in hemalaun. A washing step with aqua dest. followed. The third step was the incubation in Scott´s Solution (Sott). This is a reagent that blues hematoxylin gently. The tissue was washed again with aqua dest. Afterwards the staining with Eosin was accomplished and then washed again with aqua dest. In a last step the samples were dehydrogenized. The time of incubation was two minutes in each chemical solution.

After the staining procedure the tissue stainings were covered with Eukitt in another machine (CV5030, Leica Microsystems, Switzerland). Eukitt is a mounting medium that prevents moisture from developing under the cover glass.

The tissue samples were ready to evaluate under the light microscope.

Staining cycle: Products:

Xylol(4x)   hemalaun: 290 ml Papanicolaous
ethanol 100 %   290 ml aqua dest.
ethanol 96 %   ⎤ deparaffinization
ethanol 80 %   ⎦   Eosin: 150 ml 5 % eosin
aqua dest.   1 ml 100 % acetic acid
hemalaun (2x)   up to 580 ml with aqua dest.
aqua dest.

Sott (2x)
aqua dest.
eosin (2x)
aqua dest
ethanol 96 % (2x) ⎤
ethanol 100 % (2x) ⎬ dehydration
EBE (=n-butyl acetate) ⎦

Dyes:

Papanicolaous 1A	1092532500 Merck Millipore, Germany
Eosin 5 %	Sigma-ALD, Germany
Sott	11241, Morphisto, Germany

6.4. Immunohistochemistry

Using the immunohistochemistry (IHC) the prostate samples of the 5 different genotypes (wildtype, $PTEN^{pc+/-}$, $PTEN^{pc-/-}$, $PTEN^{pc+/-}$ $cJun^{pc-/-}$ $JunB^{pc+/-}$ and $PTEN^{pc+/-}$ $cJun^{pc+/-}$ $JunB^{pc-/-}$) were analyzed regarding 4 different targets (Androgen Receptor, cJun, JunB and ki67). All tissue slides undergoing analysis for the same target were equally treated at the same time to achieve a comparable result. For wt, $PTEN^{pc+/-}$, and $PTEN^{pc-/-}$ 5 tissue samples were available, for $PTEN^{pc+/-}$ $cJun^{pc-/-}$ $JunB^{pc+/-}$ 4 tissue samples were available and for $PTEN^{pc+/-}$ $cJun^{pc+/-}$ $JunB^{pc-/-}$ only 1 tissue sample was available for comparison during the time of the thesis was performed.

6.4.1. Deparaffinization and Rehydration

For immunohistochemical staining the slides were incubated at 56 °C for 1 h. They were then place in 100 % Xylol twice for approximately 15 min to deparaffinize the sections. To rehydrate the samples, they were incubated in an ethanol series (2x 100 %, 1x 96 %, 1x 70 %, 1x 50 %) and twice in aqua dest. for two minutes.

6.4.2. Pretreatment

This step is important to disconnect the protein cross-linkings which occurred during the formalin fixation. After this process antibodies will be able to bind to epitopes of the sample proteins.

The slides were placed into cuvettes with a special buffer and heated. Which buffers and heating methods are used in the pretreatment depends on the particular antibody. The antibodies used, their concentration and their particular pretreatment are shown in the table below. After heating, the slides were cooled down at room

temperature. They were then washed three times with phosphate buffered saline (PBS).

antibody	concentration	buffer	heating Methode
cJun CS 9165	1:100	(S2369)Citrate pH6, Dako, Denmark	Autoclave
JunB SC-46	1:300	(S2367) Tris EDTA pH9)Dako, Denmark	Steamer
AR SC-816	1:300	(S2367) Tris EDTA pH9)Dako, Denmark	Steamer
Ki67 novocastra 6002374	1:1000	(S2369) Citrate pH6, Dako, Denmark	Autoclave

Table 4: Used antibodies and their conditions for IHC. CS: Cell Signaling Technology (Massachusetts, USA); Novocastra: Leica Microsystems (Switzerland); SC: Santa Cruz Biotechnology (California, USA).

To reduce nonspecific background in the tissue sections some special treatment was needed. The slides were incubated in 3 % hydrogen peroxide for 10 min, thereby quenching the endogenous peroxidase. Afterwards the slides were washed again 3x with PBS.

6.4.3. Blocking and Antibody reaction

An Avidin-Biotin Blocking Kit (SP-2001, Vector Laboratories Inc, California, USA) was used to reduce the binding of avidin or other components of the Avidin-Biotin System. These binding processes can be due to endogenous biotin or biotin binding proteins. AvidinD solution was added dropwise on the slides and incubated for 10 min. After incubation the slides were washed 3x with PBS-Tween. Then the biotin solution was added dropwise on the slides and incubated for 10 min

A last blocking step and the following steps were accomplished with the IDetect Universal Mouse Kit (HRP) (IDSTM003, ID-Labs Inc, Ontario, Canada). A super block for 7 minutes and a universal mouse block for 1 h were done. After both blocking sessions the slides were washed 3x with PBS-Tween.

Thereafter the primary antibody was added similarly on the slides and incubated over night at 4 °C. The primary antibodies were diluted in PBS + 1 % BSA to reach the specific concentration (see table 2).

The slides were washed with PBS-Tween. Then the secondary biotinylated (anti polyvalent) antibody was added dropwise on the slides and incubated for 10 min

at room temperature. The slides were washed again with PBS-Tween.

Horse radish peroxidase (HRP) was added on the slides, incubated for another 10 min at room temperature and washed 3x with PBS-Tween.

6.4.4. Emerging

For emerging of the first slide a sample with an expected positive signal was taken. 150 µl of the Chromogen/H_2O_2 solution (AEC Chromogen Kit, 17515 ID Labs Inc., Ontario, Canada) was added. H_2O_2 acts as a substrate of HRP. This enzyme catalyzes the reaction of the colorless 3-Amino-9-Ethylcarbazole (AEC) to its red end product.
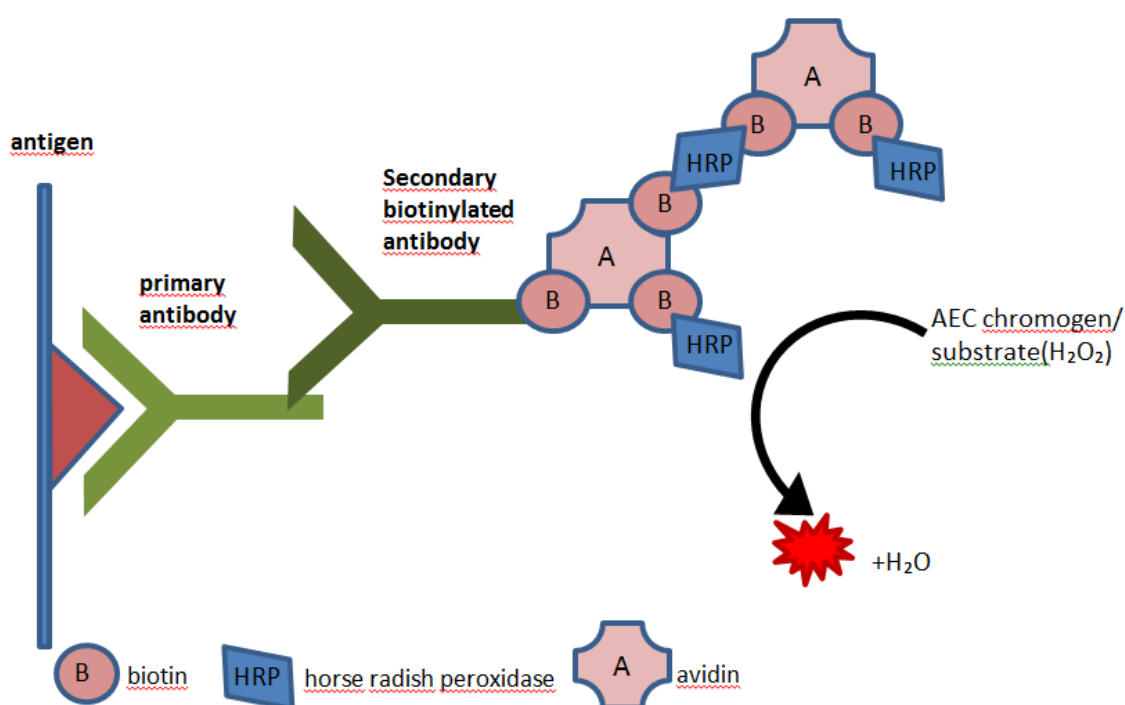
Figure 16: Scheme of the functionality of the IHC reaction. After pretreatment and blocking reactions, the antigen is treated with the primary and secondary antibody. The second antibody is biotynilated and marked with HRP. This enzyme in turn catalyzes the reaction of colorless AEC chromogen to the red end product. The amount of conversion corresponding to the intensity of the red product can be evaluated under the microscope or with special software like Histoquest[TM] [modified from http://www.piercenet.com/browse.cfm?fldID=5E9905AB-CA02-E370-95DE-C9816CF9F7DC].

The time until a strong positive red signal was perceived under the light microscope was clocked and was then used as standard timeframe for all other slides treated with this antibody. After incubation with Chromogen solution the slides were placed in aqua dest. to stop the reaction.

6.4.5. Counterstaining

After the immunohistochemical staining of the target antigen the slides were stained a second time with Meyer's hemalaun (1:5 diluted with aqua dest., 1.09249.0500, Merck, Germany) to get a better contrast.

The slides were incubated with the Hemalaun solution for some seconds and then washed with water immediately. The result was monitored under the light microscope. This process was repeated until an optimal contrast was achieved.

After finishing the staining of the slides they were covered with Aquatex (108562, Merck, Germany) and a cover slip. The samples were then ready for analyzing and were stored at room temperature.

10x PBS pH 7,5	PBS-Tween
28.8 g Na_2HPO_4 $2H_2O$	100 ml 10x PBS
5.2 g NaH_2PO_4 H_2O	0.25 % Tween20
90 g NaCl	
filled up with a. d. to 1 l	filled up with a. d. to 1 l

6.4.6. Histoquest

Histoquest[TM] (Tissuegnostics[TM]) is a software program for quantification of proteins from IHC stained slides. Thus it is easily possible to quantify protein expression levels and compare the different groups (genotypes) regarding these observations.

cJun, JunB, ki67 and androgen receptor expressing cells were defined for each staining regimen. Cells can be analyzed with different parameters such as color intensity or diameter. For these prostate samples it was also necessary to define the specific area in the photo that should be analyzed, because the prostate is a very heterogeneous tissue and the risk for false negative cells should be minimized. After analysis all data were shown in a report.

For each sample a ratio of all positive cells to all analyzed cells was calculated. For each staining with 5 mice, with 3 pictures each, mean values were calculated. With these means an unpaired T-test was done for each staining group. If the P-value was under 0.05 the mean values of the various groups (genotypes) were considered to differ

significantly. For cre+ PTEN fl/+ cJun fl/+ JunB fl/fl with one sample, a statistical analysis with Histoquest^{TM} was not feasible.

The coefficient of variation (C_v) was not calculated for the results of the Histoquest^{TM} program. In some cases of the IHC experiments the means of the expression levels were nearing zero and therefore the C_v is not useful. For the C_v to be meaningful the means have to be rather high, otherwise also a small standard deviation can cause an immense c_v even when the difference is minimal.

6.5. Western Blot

6.5.1. Protein Lysates

For preparing the protein lysates from the prostate samples that were stored at -80 °C, IP-buffer + Inhibitors were used. The frozen prostate tissue was placed into a douncer and 250 μl IP-buffer + Inhibitors was added. The prostate sample was dounced until it was homogenized. The whole douncing process was done on ice. After homogenization the sample was shaken for 1 h at 4 °C and then centrifuged for 30 min at 4 °C at 13000 rpm (15682 x g). The supernatant was taken and centrifuged a second time for 20 min at 4 °C at 13000 rpm (15682 x g). After this step the supernatant was ready to use for western blotting or, alternatively, stored at -80 °C.

IP-buffer	IP-buffer with Inhibitors
25 mM HEPES pH7.5	1 ml IP-buffer
150 mM NaCl	40 μl Protease Inhibitors
10 mM EDTA pH8	10 μl Aprotinin 1 mg/ml
10 mM beta glycerolphosphate	10 μl PMSF 100 mM
0.1 % Tween 20	2 μl NaF 500 mM
0.5 % NP-40	10 μl Na Van 100 mM
stored at room temperature	1 μl Leupeptin 1 μg/μl
	freshly prepared on ice

6.5.2. Protein Concentration with Bradford Assay

To measure the protein concentration of the prostate samples the Pierce Coomassie Plus (Bradford) Protein Assay (Thermo Scientific, Massachusetts, USA) was used. This is

a calorimetric protein assay based on the dye Coomassie Brilliant blue G-250. Under acidic conditions and in occurrence of proteins the red form of the dye is converted to its blue form. The colorimetric measurement was done with a spectrophotometer (U-2000, Hitachi, Japan) at 595 nm. To interpret the results a BSA standard line was prepared and measured right before the prostate samples.

6.5.3. Western Blotting

For Western Blotting 40 µg of sample protein was loaded. Therefore the following calculation was used. The desired amount of protein (40 µg) was divided by the protein lysate concentration in µg/µl measured with the Bradford Assay. The calculated amount of protein lysate (in µl) was filled up to 5 µl with IP-buffer + Inhibitors. In the next step 5 µl Laemmli sample buffer (2x SDS gel-loading dye) was added. The ratio of protein lysates with IP-buffer/ sample buffer is 1:1. This solution was heated up to 95 °C for 7 min. After heating, the samples were put on ice and centrifuged briefly. The complete 10 µl were applied on the gel. The gel is a 5-15 % Tris-Glycine SDS-Polyacrylamide gel. The gel was run at 120 V in electrophoresis buffer. To interpret the bands a prestained protein ladder (Thermo Scientific, Massachusetts, USA) was used. After electrophoresis the gel and a piece of nitrocellulose (Merck Millipore, Germany) was put in a transfer chamber. The exact arrangement for this transfer sandwich is shown in the illustration below. The transfer was run over night at 20 V in a 20 % methanol transfer buffer.

<u>2x SDS gel-loading dye</u>   <u>Transfer Arrangement</u>

100 mM Tris-HCL pH 6,8
200 mM DTT
4 % SDS
20 % Glycerol

20 mg Bromphenol blue
filled up to 20 ml with aqua dest.
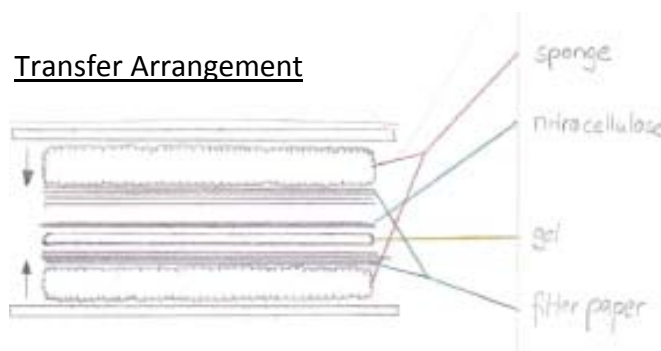
Electrophoresis buffer   Transfer buffer

144 g Glycine   112 g Glycine
30 g Tris   24.5 g Tris
10 g SDS   20 % Methanol
filled up to 10 l with aqua dest.   filled up to 10 l with aqua dest.

TBS-T pH 7.5   Ponceau solution

6.5 g Tris   0.1 % Ponceau
9 g NaCl   5 % Acetic acid
0.1 % Tween 20
filled up to 1 l with aqua dest.

After transferring the proteins onto the nitrocellulose all proteins were stained with Ponceau solution to check if the transfer was successful. The Ponceau solution was then washed off with TBS-T for 10 min.

In the next step the proteins were blocked with 5 % dry milk in TBS-T for 1 h at room temperature. After blocking the nitrocellulose was washed again with TBS-T for 15 min. The nitrocellulose was incubated with primary antibody over night at 4 °C while shaking. As loading control a beta actin antibody was used. The primary antibody was then removed and the nitrocellulose was washed with TBS-T for 30 min while shaking.

The exact information on primary antibodies, used concentrations and their particular secondary antibodies can be looked up in the table below.

Primary Antibody	Company	Concentration	Secondary Antibody
Beta Actin	CS 4967	1:1000	anti rabbit
cJun	SC 1694	1:200	anti rabbit
JunB	SC 73X	1:2000	anti rabbit
Androgen Receptor	SC 816	1:1000	anti rabbit
p16	SC 74401	1:200	anti mouse
p21	SC 397	1:1000	anti rabbit
p27	SC 1641	1:200	anti mouse
PTEN	CS 9559	1:1000	anti rabbit
p-serAkt	CS 4058	1:1000	anti rabbit
Pan Akt	CS 4685	1:1000	anti rabbit

Table 5 Used antibodies and their conditions for WB. CS: Cell Signaling Technology (Massachusetts, USA); SC: Santa Cruz Biotechnology (California, USA).

The nitrocellulose was then incubated with the secondary antibody for 1 h at room temperature while shaking. The concentration for the secondary antibody was 1:5000 in TBS-T. After 1 h incubation the secondary antibody was removed and the nitrocellulose was washed a last time with TBS-T for 45 min.

For visualization of the immune reaction the ECL Plus Western Blotting Detection System (GE Healthcare, UK) was used. Both solutions were poured on the nitrocellulose and after 5 min incubation time the chemiluminescent signal (Luminol) was analyzed with a LUMI Imager F1 (Boehringer, Germany).
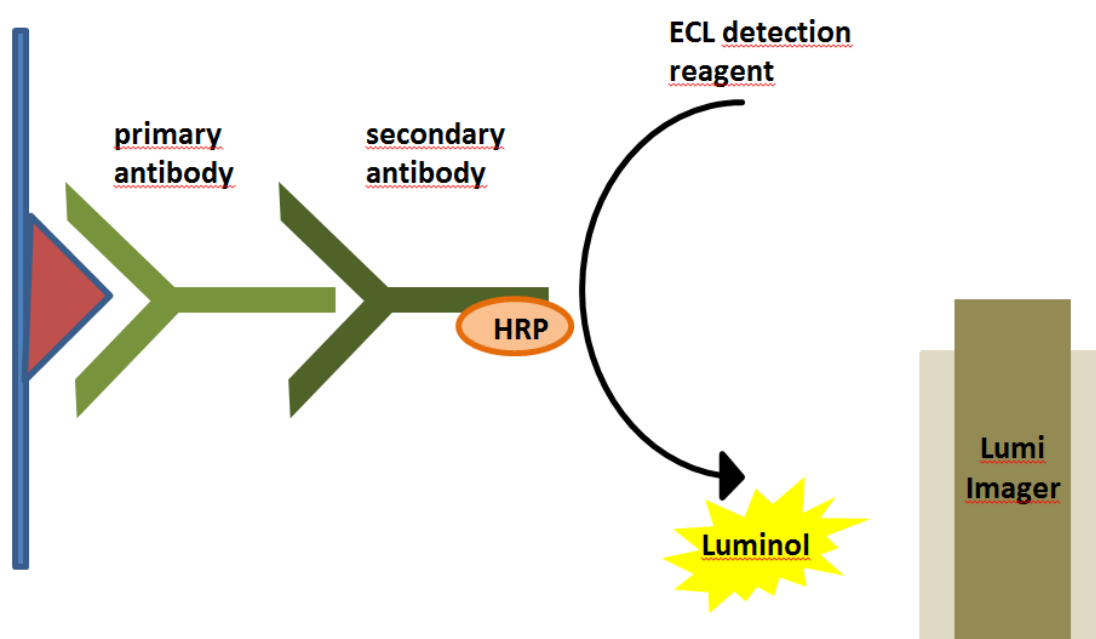
Figure 17: Scheme of the functionality of the WB reaction. After transferring, the antigen is located on nitrocellulose and treated with primary and secondary antibody. The second antibody is marked with HRP that in turn catalyzes the reaction with the ECL detection reagent to Luminol. The amount of conversion corresponds to the intensity of Luminol, which is then detected by a Lumi Imager [modified from http://www.crbdiscovery.com/newsletter/MAY.html].

7. Results

7.1. Breeding

In the first breeding PTEN$^{pc+/-}$ and PTEN$^{pc-/-}$ mice were generated. The bodyweight, the weight of the prostate tissue, and images of the whole prostate were compared between wt, PTEN$^{pc+/-}$ and PTEN$^{pc-/-}$ prostate samples.

The comparison of the body weight analyzed with an unpaired T-Test showed no significant differences between the genotypes (Figure 18). The bodyweight in PTEN$^{pc+/-}$ and PTEN$^{pc-/-}$ mice was slightly higher than the bodyweight in wt mice.

A significant difference was detected in the weight of the prostate tissue. In PTEN$^{pc-/-}$ mice the prostate was enlarged compared to wt and PTEN$^{pc+/-}$ prostates (Figure 19). No difference could be found in the prostate weight of wt mice as compared to PTEN$^{pc+/-}$ mice. The coefficient of variation for each column (mouse bodyweight and prostate weight) was always below 0.5, or 50% respectively. That shows that the determined means typify all data (Table 6).
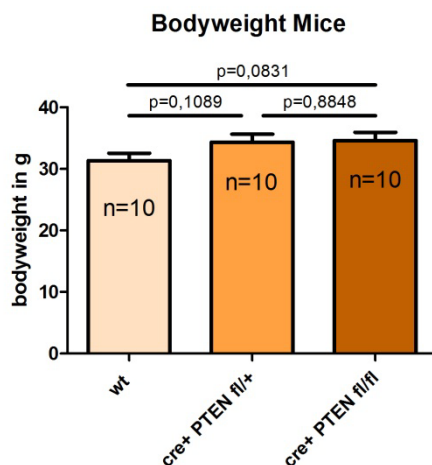
Figure 19: Statistical Analysis of the mouse bodyweight by an unpaired T-Test shown with bar graphs. No significant differences in the means of the bodyweight could be detected between wt, PTEN$^{pc+/-}$ and PTEN$^{pc-/-}$.
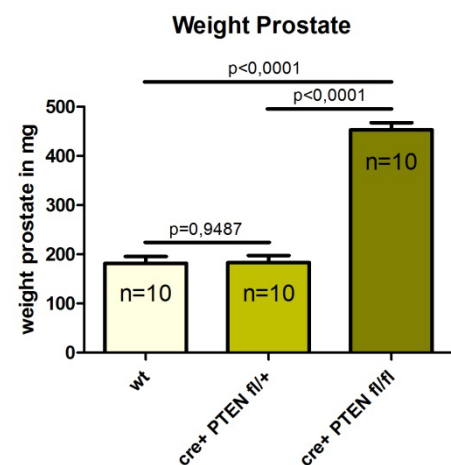

Figure 18: Statistical Analysis of the mouse prostate weight by an unpaired T-Test shown with bar graphs. PTEN knockout prostate samples were significantly bigger than wt and PTEN$^{pc+/-}$ prostate samples.

Bodyweight   **Weight**

Mice   **Prostate**

	wt	PTEN^{pc+/-}	PTEN^{pc-/-}		wt	PTEN^{pc+/-}	PTEN^{pc-/-}
Mean ($\overline{x}$)	31.35 g	34.34 g	34.62 g	Mean ($\overline{x}$)	181.8 mg	183.1 mg	453.0 mg
Std. Deviation (SD)	3.771	4.156	4.183	Std. Deviation (SD)	43.23	45.86	46.20
Coefficient of Variation (C_V)	**12.0%**	**12.1%**	**12.1%**	Coefficient of Variation (C_V)	**23.8%**	**25.0%**	**10.2%**

Table 6: Coefficient of Variation (C_v) shown for wt, PTEN^{pc+/-}and PTEN^{pc-/-} respectively for the mouse bodyweight and the weight of the mouse prostate. The C_v was always under 50%, which demonstrates, that the means typify the data.

The difference in prostate size was also noticeable in the prostate images. The prostate tissue of PTEN^{pc-/-} was enlarged as compared to wt and PTEN^{pc+/-}. Between wt and PTEN^{pc+/-} no significant macroscopic differences were observed (Figure 20).

Figure 20: Macroscopic images of the urogenital tract of mice. The prostate of PTEN knockout mice (c) is enlarged as compared to the wildtype (a) and the cre+ PTEN fl/+ (b) prostates.

The PTEN^{pc-/-} mice were intercrossed with cJun and JunB floxed mice.

For PTEN the offspring always showed the genotype of Δ/+. The Delta allele results from a PTEN knock out in the whole organism and was determined by PCR genotyping. The genotypes for JunB and cJun did not always occur in the expected Mendelian frequency. For cJun this is shown in Figure 21. Just double bands representing the fl/+ genotype should have occurred, but single upper bands (fl/fl) and single lower bands (+/+) were also visible.
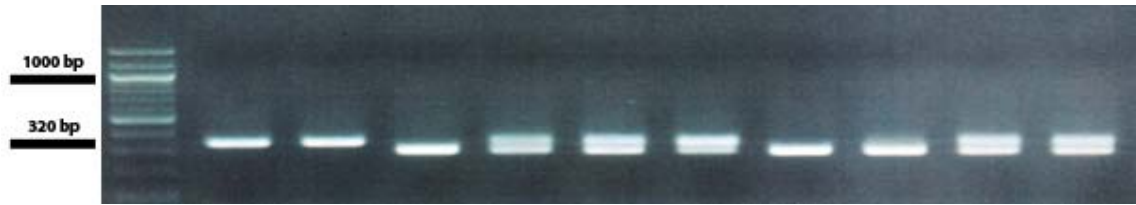
Figure 21: Results of the PCR for the cJun genotyping with a 2% Agarose gel and Midori Green using a 100 bp ladder (Lane1). The floxed cJun band is shown at 320bp (Lane 2) and the wt cJun band at 280bp (Lane 4). Only double bands should appear, showing fl/+ genotypes, yet we found a mixture of fl/fl, fl/+ and +/+ genotypes.

To generate the PTEN cJun and/or JunB knockouts only mice with the expected fl/+ or Δ/+ were used for breeding. The resulting generation offered various genotypes but no cJun, JunB double knockout and no cJun or JunB single knockout mice. Also for PTEN no homozygote knockout was recognized. For further experiments male mice with the following genotypes were analyzed: cre+ PTEN fl/+ with cJun fl/+ JunB fl/+ or cJun fl/fl JunB fl/+ or cJun fl/+ JunB fl/fl.
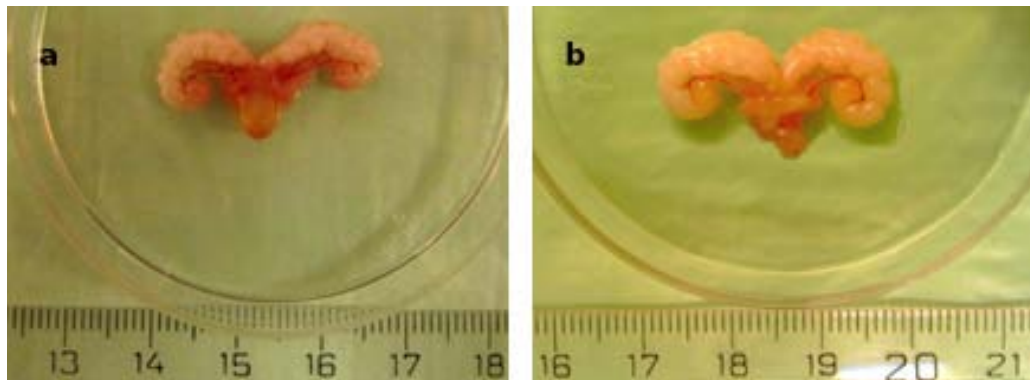
Figure 22: Macroscopic images of the urogenital tract of mice. No differences were found between the prostates of the PTEN$^{pc+/-}$cJun$^{pc-/-}$JunB$^{pc+/-}$ (a) and the PTEN$^{pc+/-}$cJun$^{pc+/-}$JunB$^{pc-/-}$ (b) mice. There were also no differences between the prostates in this table and the wt and PTEN$^{pc+/-}$ prostates shown in Figure 20. Especially no enlargement was observed like in the PTEN$^{pc-/-}$prostates.

The number of mice per genotype was too small to give statistically relevant data (4 mice with cJun$^{-/-}$ JunB$^{+/-}$ and 1 mouse with cJun$^{+/-}$JunB$^{-/-}$), but it seems that the body- and the prostate weight are comparable with the wt and PTEN$^{pc+/-}$. Additionally the macroscopic images showed that the prostates of cJun and JunB knockouts are comparable to the wt and PTEN$^{pc+/-}$. A massive enlargement of the prostate, as observed in PTEN$^{pc-/-}$, could not be observed (Figure 22).

7.2.   HE's

Analysis of the HE staining showed the characteristic histological differences between wt, PTEN$^{pc+/-}$ and PTEN$^{pc-/-}$ prostate tissue. Characteristic signs are marked with an arrow in the images of Figure 23.

The normal prostate tissue was found in wt mice. The PTEN$^{pc+/-}$ mice showed precancerous signs like those found in human prostatic intraepithelial neoplasia, either as low grade PIN (LGPIN) or high grade PIN (HGPIN). The cytological changes of PIN are characterized by presence of nucleoli, increase of nuclear to cytoplasmic ratio and increased nuclear size. (24c).The secretory cell layers showed signs of intraluminal papillary proliferation (24d) and only few residual basal cells were recognized.

In the PTEN knockout mice LGPIN, HGPIN and prostate cancer formation were identified. In some regions the basal layer was absent (24e). In such regions an invasion into the stroma or luminal fusion was observed (24f). Enlarged nuclei and many prominent nucleoli were observed, too.

Most precancerous and cancer incidences were seen in the PTEN$^{pc-/-}$ mice, whereas in PTEN$^{pc+/-}$ mice only precancerous lesions were observed.

In the second breeding HE stainings were done for PTEN$^{pc+/-}$cJun$^{pc+/-}$; PTEN$^{pc+/-}$cJun$^{pc-/-}$ JunB$^{pc+/-}$ and PTEN$^{pc+/-}$cJun$^{pc+/-}$JunB$^{pc-/-}$.

Similar histological change was found comparing PTEN$^{pc+/-}$cJun$^{pc+/-}$ with PTEN$^{pc+/-}$. The intraluminal proliferation of the secretory cells in PTEN$^{pc+/-}$cJun$^{pc+/-}$ was as pronounced as in PTEN$^{pc+/-}$ (24c, d and 25a, b).

In PTEN$^{pc+/-}$cJun$^{pc-/-}$JunB$^{pc+/-}$ signs of LGPIN, HGPIN and Prostate Cancer were identified. The severity of histological changes was as pronounced as in PTEN$^{pc-/-}$. The area of intraluminal proliferations was larger in PTEN$^{pc+/-}$cJun$^{pc-/-}$JunB$^{pc+/-}$ as compared to PTEN$^{pc-/-}$ mice (25c and 24e).

No histological change was found comparing PTEN$^{pc+/-}$cJun$^{pc+/-}$JunB$^{pc-/-}$ with PTEN$^{pc+/-}$. The level of intraluminal proliferation of secretory cells and also their cytological changes were comparable to PTEN$^{pc+/-}$ (24c, d and 25e, f).

Figure 23: HE stainings show characteristic histological differences in the prostate tissue of wt (a, b), PTEN$^{pc+/-}$ (c, d) and PTEN$^{pc-/-}$ (e, f) mice (scale bar 50µm). Characteristic signs are shown with an arrow. In wt with normal prostate tissue a connective tissue between adjacent glands and uniform nuclei are visible (arrows 24a). Many basal cells surround the glands (24b). In PTEN$^{pc+/-}$ precancerous signs like presence of nucleoli, increase of nuclear to cytoplasmic ratio and increased nuclear size (24c) and the beginning of intraluminal papillary proliferations (24d) are visible. In PTEN knockout prostate tissue prostate cancer marks like massive intraluminal proliferation (24e), an absent basal layer (24e) and luminal fusion of the glands (24f) are visible.
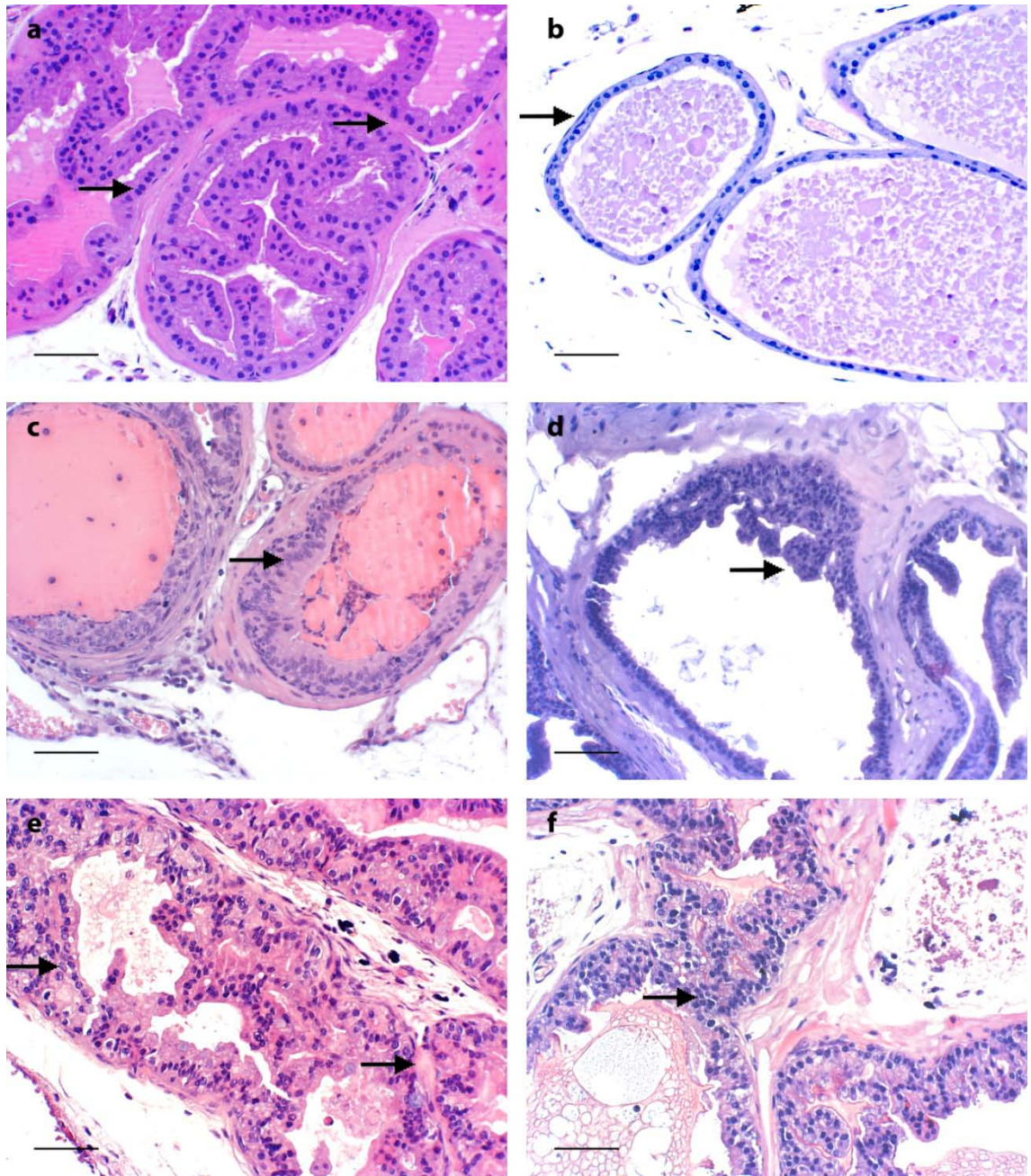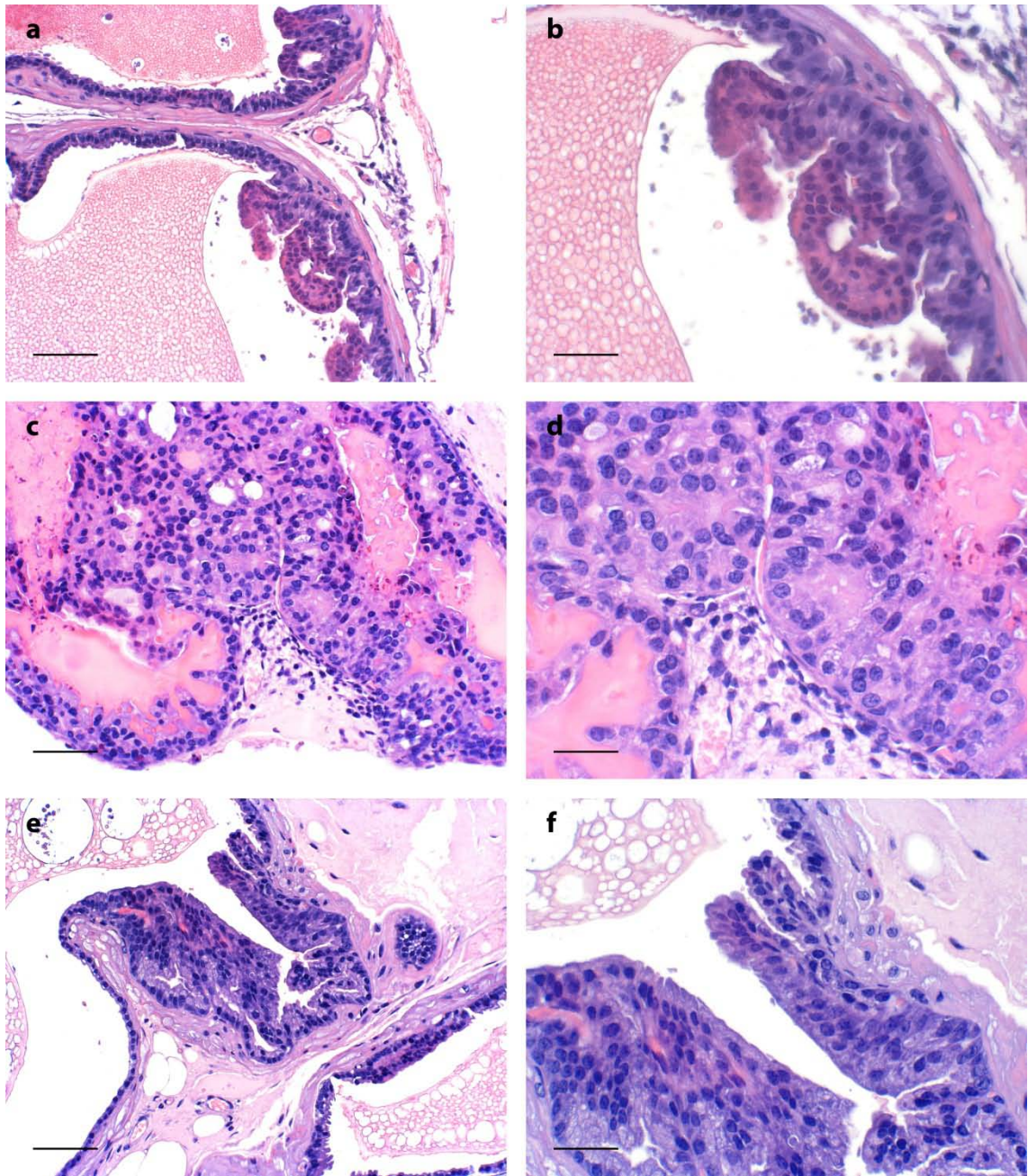
Figure 24: HE stainings show characteristic histological differences in the prostate tissue of PTEN^pc+/- cJun^pc+/- (a, b), PTEN^pc+/-cJun^pc-/-JunB^pc+/- (c, d) and PTEN^pc+/-cJun^pc+/-JunB^pc-/- mice (scale bar left side 50μm, right side 25μm). Similar histological alterations were found comparing PTEN^pc+/-cJun^pc+/- and PTEN^pc+/-cJun^pc+/-JunB^pc-/- and PTEN^pc+/- (Figure 23c, d). Signs of massive intraluminal proliferation of secretory cells in cre+ PTEN^pc+/-cJun^pc-/-JunB^pc+/- (25c) were more pronounced compared to PTEN^pc-/- (24e).

7.3.   IHC

7.3.1. Androgen Receptor

There was no significant change in the expression of Androgen Receptor in wt and PTEN$^{pc+/-}$. In the mean value PTEN$^{pc+/-}$ prostate tissue showed 2% higher AR activity than the wt prostate tissue (wt: 27.2 % and PTEN$^{pc+/-}$: 29.2%).
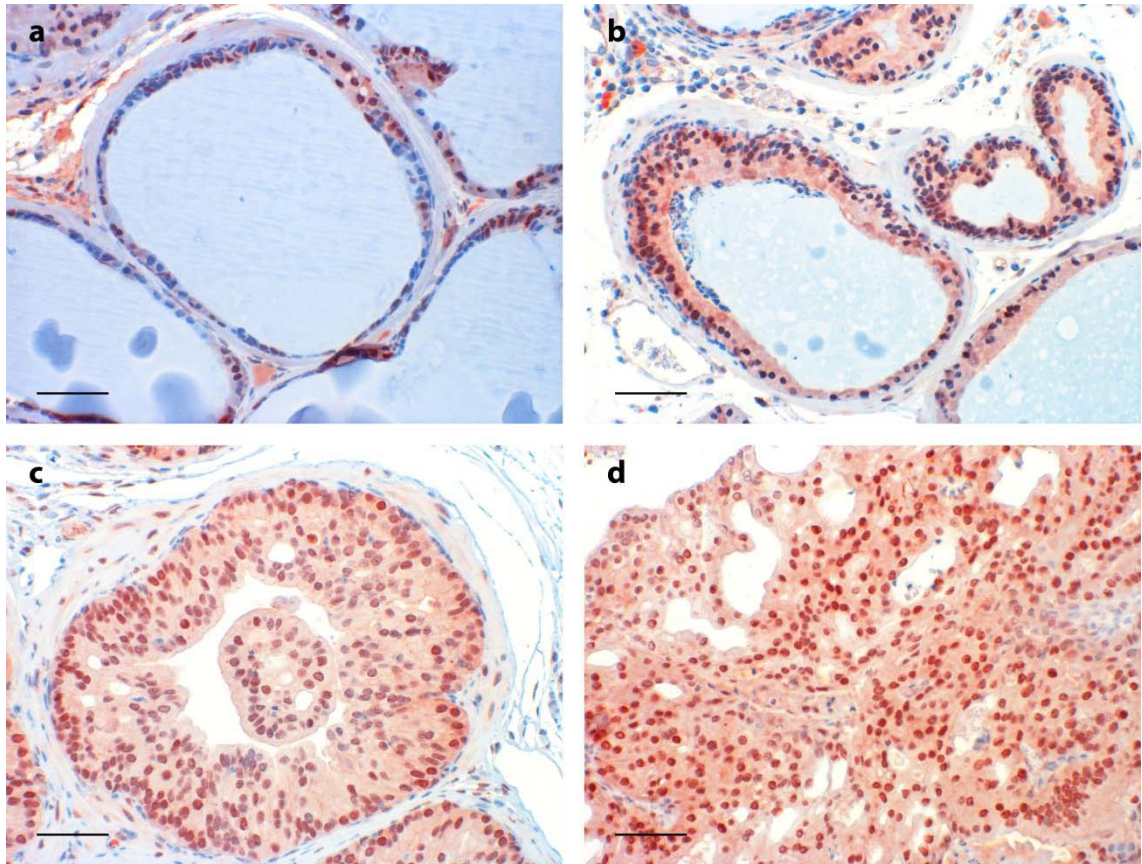
Figure 25: Images of the IHC staining of mice prostates tissue for Androgen Receptor (scale bar 50 μm). Blue=nuclear hemalaun counterstaining, red=AR nuclear + cytoplasm. The highest AR activation was seen in PTEN$^{pc+/-}$cJun$^{pc-/-}$JunB$^{pc+/-}$ and PTEN$^{pc-/-}$ mice, and intermediate AR expression level in PTEN$^{pc+/-}$ mice. The least AR activity was recognized in wt samples.

A massive increase in AR activation was measured in PTEN$^{pc-/-}$ and PTEN$^{pc+/-}$cJun$^{pc-/-}$ JunB$^{pc+/-}$ prostates. Both genotypes showed an expression of AR in about 80% of cells, but the highest expression was observed in the cJun knockout prostate tissue (PTEN$^{pc-/-}$: 77.1% and PTEN$^{pc+/-}$cJun$^{pc-/-}$JunB$^{pc+/-}$: 81.6%) (Figure 25). The AR expression was significantly higher in the PTEN knockout and PTEN$^{pc+/-}$cJun$^{pc-/-}$JunB$^{pc+/-}$ samples compared to the wt and PTEN$^{pc+/-}$ prostate samples.

Androgen Receptor

Figure 26: Comparison of theAR-expression mean values with an unpaired T-Test. Mean values from the IHC of the AR were determined with Histoquest[TM]. No differ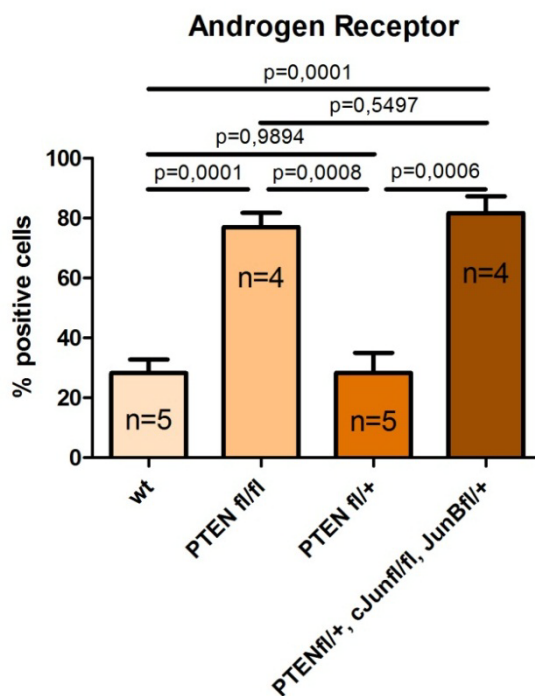ences in the AR-Expression were observed between wt and PTEN[pc+/-] prostate samples (both around 30%) and between PTEN knockout and PTEN[pc+/-]cJun[pc-/-]JunB[pc+/-] prostate samples (both around 80%). The AR-expression was significantly higher in PTEN knockout and PTEN cJun knockout samples compared to wt and PTEN[pc+/-] samples.

The expression levels of AR in PTEN[pc+/-]cJun[pc-/-]JunB[pc+/-] was more pronounced compared to PTEN[pc-/-], however not statistically significant (p=0.5497) (Figure 26).
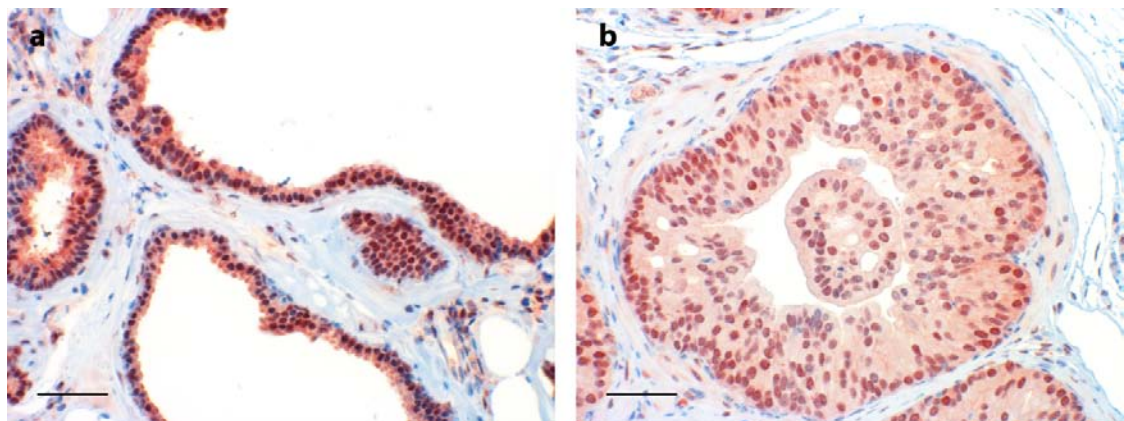
Figure 27: Image of the AR staining of the single prostate tissue sample of PTEN[pc+/-]cJun[pc+/-]JunB[pc-/-] (a) (scale bar 50μm). Blue=nuclear hemalaun counterstaining, red=AR nuclear + cytoplasm. Its activity is a little higher compared to wt and PTEN[pc+/-] but much lower compared to PTEN[pc-/-] (b) and PTEN[pc+/-]cJun[pc-/-]JunB[pc+/-].

The AR staining of the PTEN[pc+/-]cJun[pc+/-]JunB[pc-/-] sample showed an AR activation in 35.4% of the prostate epithelial cells. This AR activity is a little higher than observed in wt and PTEN[pc+/-] but much less compared with PTEN[pc-/-] and PTEN[pc+/-]cJun[pc-/-]JunB[pc+/-] prostates (Figure 27).

7.3.2. cJun

The genotypes of wt, PTEN$^{pc+/-}$ and PTEN$^{pc+/-}$cJun$^{pc-/-}$JunB$^{pc+/-}$ showed almost no detectable cJun expression. Only very few positive cells using cJun Abs were recognized.

In prostate tissue after loss of PTEN an increase of the expression of cJun up to 4.5% was recognized. However, due to low sample number the difference between PTEN knockout samples and wt, PTEN$^{pc+/-}$ and PTEN$^{pc+/-}$cJun$^{pc-/-}$JunB$^{pc+/-}$ was not statistically significant (Figure 28, Figure 29).
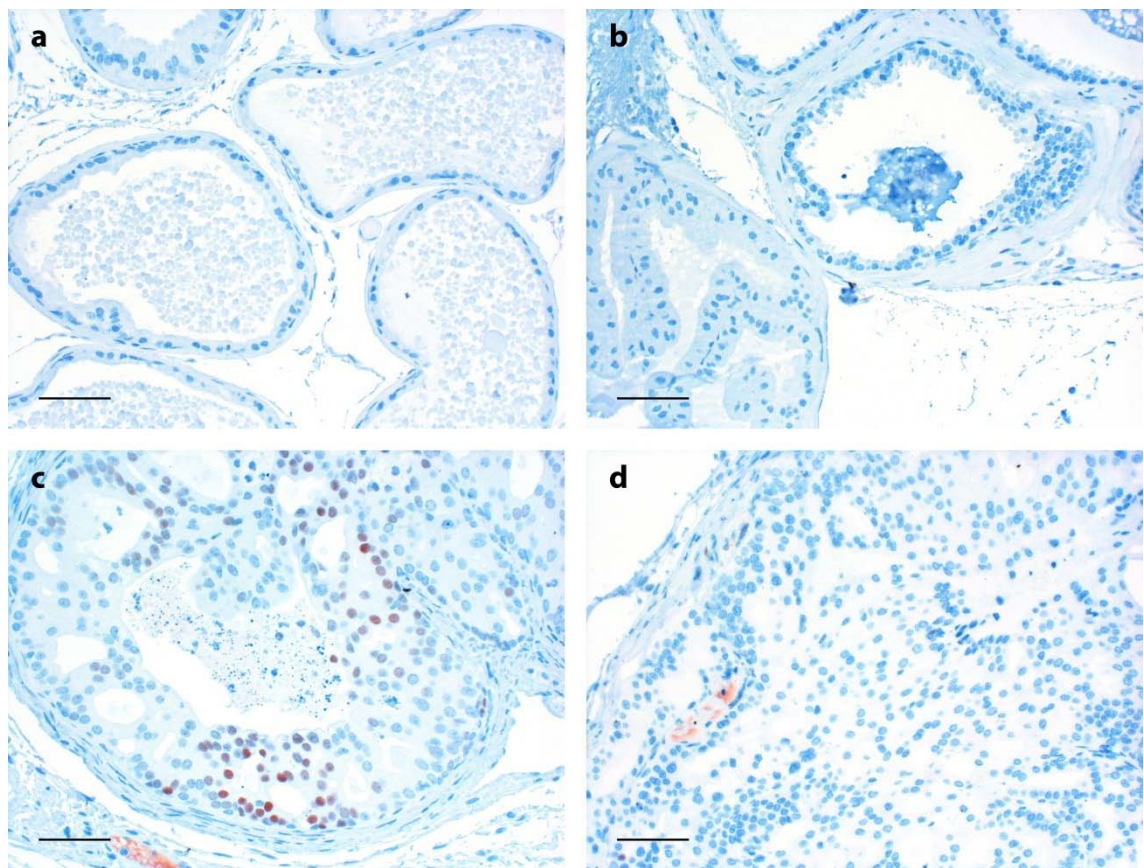

Figure 28: Images of the IHC staining of mice prostate tissue cJun (scale bar 50 µm). Blue=nuclear hemalaun counterstaining, red=cJun nuclear + cytoplasm. Almost no cJun expression was detectable in wt (a), PTEN$^{pc+/-}$ (b) and PTEN$^{pc+/-}$cJun$^{pc-/-}$JunB$^{pc+/-}$ (d). In PTEN$^{pc-/-}$ (c) the cJun activity was highly increased.
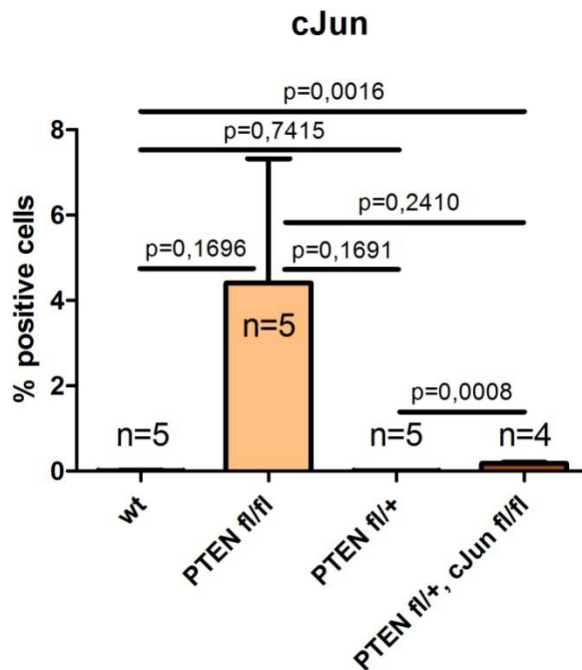
Figure 29: Comparison of the cJun expression mean values with an unpaired T-Test. Almost no cJun expression was detectable in wt, PTEN[pc+/-] and PTEN[pc+/-]cJun[pc-/-]JunB[pc+/-]. The cJun expression was increased in PTEN[pc-/-] prostate tissue. However, the cJun expression was not significantly different to wt, PTEN[pc+/-] and PTEN[pc+/-]cJun[pc-/-]JunB[pc+/-].

The cJun staining of the PTEN[pc+/-]cJun[pc+/-]JunB[pc-/-] sample showed 5% cJun positive cells. The observed cJun activity was as high as the cJun activity in PTEN[pc-/-] (Figure 30).
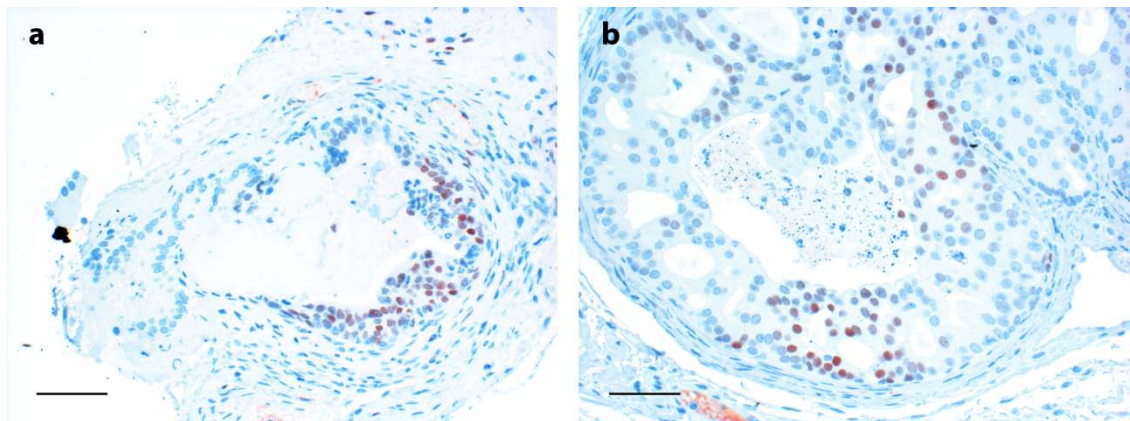
Figure 30: Image of the cJun staining of the single prostate tissue sample of PTEN[pc+/-]cJun[pc+/-]JunB[pc-/-] (a) (scale bar 50 µm). Blue=nuclear hemalaun counterstaining, red=cJun nuclear + cytoplasm. The cJun activity of PTEN[pc+/-]cJun[pc+/-]JunB[pc-/-] was as high as in PTEN[pc-/-] (b).

When looking at the data for the cJun stained samples, a qualitative approach seems indicated, possibly even more than a quantitative approach. Therefore, an unpaired t-test analysis was done comparing the number of samples that include cells with high cJun expressions in the IHC. In total numbers these were 0/5 samples in the wildtype group, 4/5 samples in the PTEN[pc-/-] group, 0/5 samples in the PTEN[pc+/-] group, and 0/4

samples in the PTEN$^{pc+/-}$cJun$^{pc-/-}$JunB$^{pc+/-}$ group. After manually going through the slides we came to the conclusion, that the few cells, which have been marked in the IHC of the PTEN$^{pc+/-}$cJun$^{pc-/-}$JunB$^{pc+/-}$ group, did not meet the criteria of highly cJun expressing cells and must therefore, be regarded as artifacts.

The T-test showed that the differences between the PTEN$^{pc-/-}$ group and the wildtype, PTEN$^{pc+/-}$, and PTEN$^{pc+/-}$cJun$^{pc-/-}$JunB$^{pc+/-}$ groups were highly significant (p = 0.0039; 0.0039; and 0.0096 respectively) (data not shown).

7.3.3. JunB

The JunB expression analysis with IHC comparing mean values with an unpaired T-Test showed an increase from wt prostate samples with almost no JunB positive cells (0.32%) to PTEN$^{pc+/-}$ with around 2% positive cells and up to 6% positive cells in the
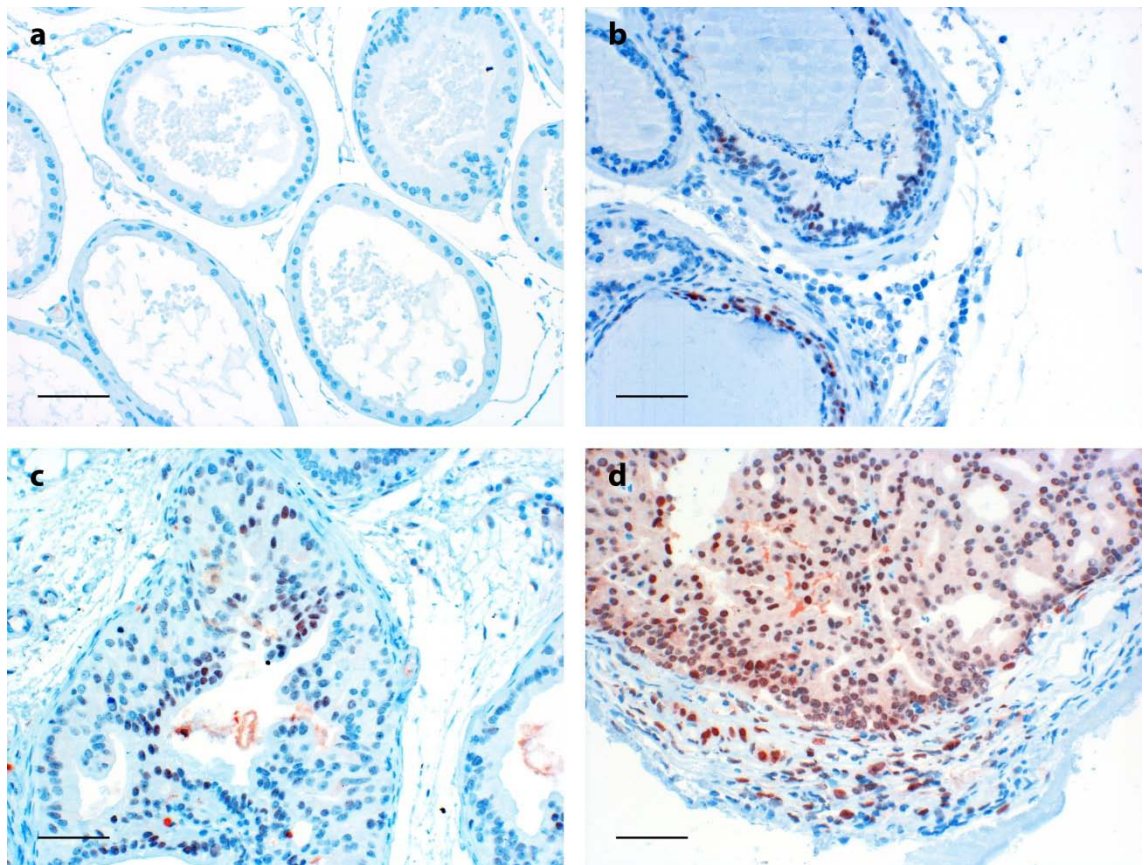
Figure 31: Images of the JunB IHC staining of mouse prostates tissue (scale bar 50 µm). Blue=nuclear hemalaun counterstaining, red=JunB nuclear + cytoplasm. A slight increase of JunB expression was observed from wt (a) with almost no JunB expression to PTEN$^{pc+/-}$ (b) with around 2% positive cells to cre+ PTEN$^{pc-/-}$ (c) with 6% JunB expression. A massive increase in the JunB expression was observed in PTEN$^{pc+/-}$cJun$^{pc-/-}$JunB$^{pc+/-}$with almost 19% JunB positive cells (d).

tumor tissue of PTEN$^{pc-/-}$. In PTEN$^{pc+/-}$cJun$^{pc-/-}$JunB$^{pc+/-}$ an elevated JunB expression of 18.9% positive cells was identified, although one allele of JunB was knocked out in this genotype (Figure 31, Figure 32).
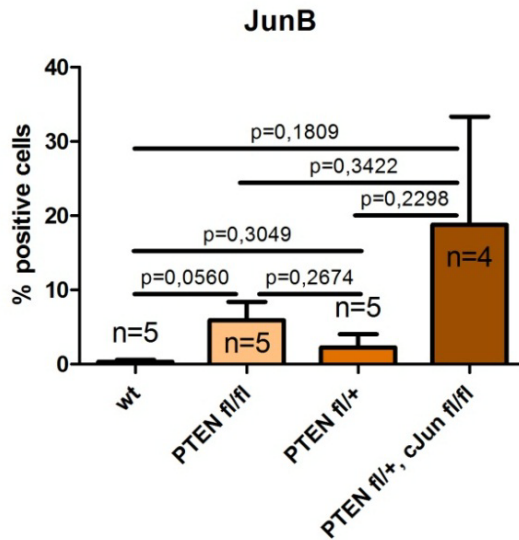
Figure 32: Comparison of the JunB mean expression values using an unpaired T-Test. JunB expression was lowest in wt-mice, slightly increased in PTEN$^{pc+/-}$and about twice as high in PTEN$^{pc-/-}$ (Yet below 10%). JunB expression was by far highest in PTEN$^{pc+/-}$cJun$^{pc-/-}$JunB$^{pc+/-}$ mice (up to 20%). However, this difference was not significant.

In the PTEN$^{pc+/-}$cJun$^{pc+/-}$JunB$^{pc-/-}$ sample the JunB staining showed no positive cells in the prostate tissue (Figure 33a).

Figure 33: Image of the JunB staining of the single prostate tissue sample of PTEN$^{pc+/-}$cJun$^{pc+/-}$JunB$^{pc-/-}$ (a) (scale bar 50 μm). Blue=nuclear hemalaun counterstaining, red=JunB nuclear + cytoplasm. JunB staining in the PTEN$^{pc+/-}$cJun$^{pc+/-}$JunB$^{pc-/-}$ mouse showed no positive cells compared to PTEN$^{pc+/-}$cJun$^{pc-/-}$JunB$^{pc+/-}$ (b) mice increased JunB expression.

7.3.4.   Ki67

A slight increase in Ki67 expression was found in PTEN$^{pc+/-}$ with 3.35% positive cells compared to wt with 3.03%. The tumor tissue of PTEN$^{pc-/-}$ showed a significantly higher ki67 activity (8.28%) compared to wt and PTEN$^{pc+/-}$. In PTEN$^{pc+/-}$cJun$^{pc-/-}$JunB$^{pc+/-}$ the activaton of ki67 was massively increased with 18.19% positive cells. However, this increase in Ki67 activation was not statistically significant compared to wt, PTEN$^{pc+/-}$ and PTEN$^{pc-/-}$ (Figure 34, Figure 35).
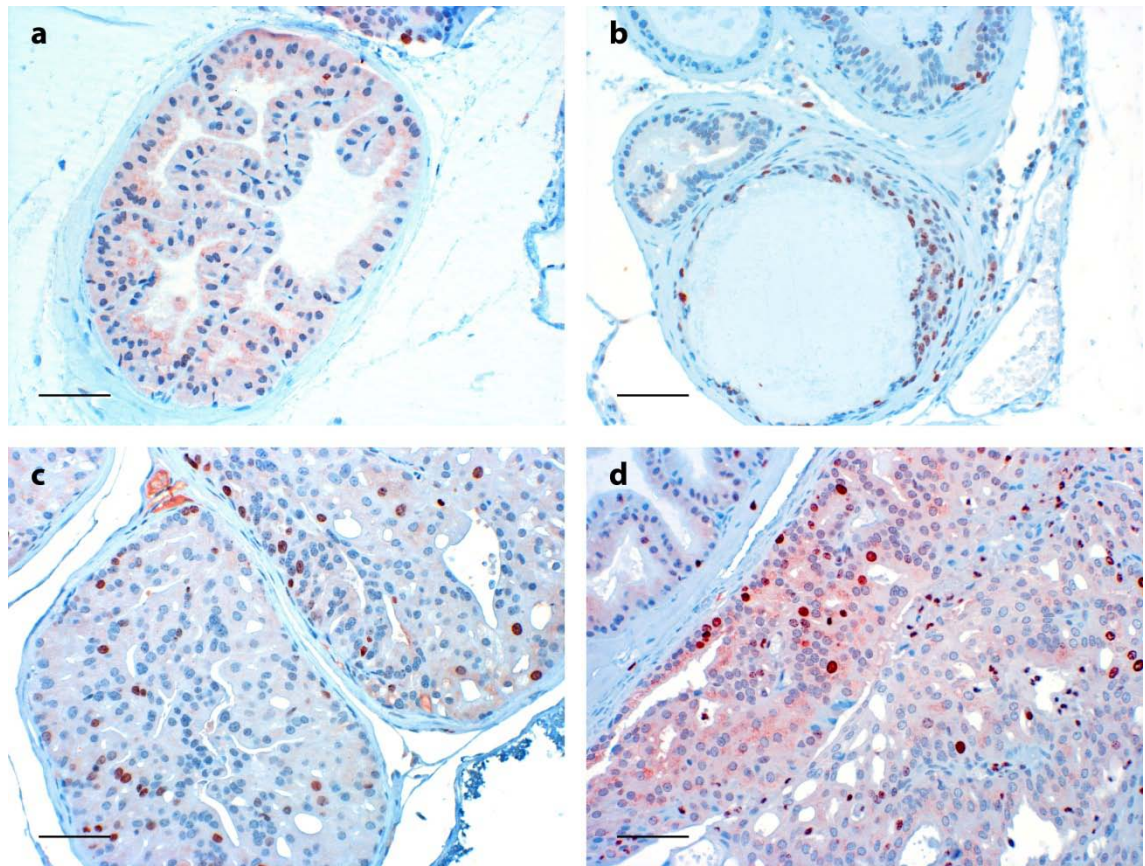
Figure 34: Images of the IHC staining of mice prostates tissue Ki67 (scale bar 50 µm). Blue=nuclear hemalaun counterstaining, red=Ki67 nuclear + cytoplasm. An increase in Ki67 expression was observed from wt (a) over PTEN$^{pc+/-}$ (b) to PTEN$^{pc-/-}$ (c). PTEN$^{pc+/-}$cJun$^{pc-/-}$JunB$^{pc+/-}$ showed the highest Ki67 activity.

ki67

In the prostate tissue of the PTEN[pc+/-]cJun[pc+/-]JunB[pc-/-] sample a low activity of ki67 (1.58%) was detected. The expression level was lower than observed in wt and PTEN[pc+/-] (Figure 36).
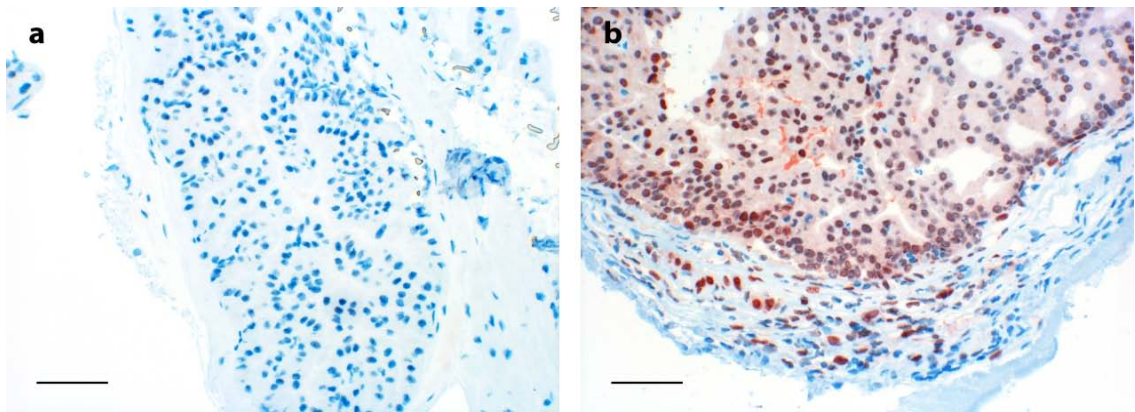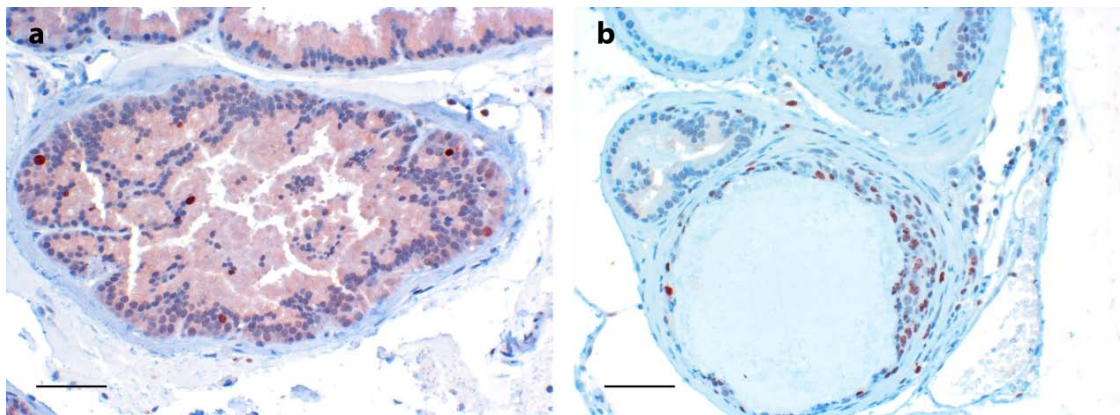

Figure 36: Image of the Ki67 staining of the single prostate tissue sample of PTEN[pc+/-]cJun[pc+/-] JunB[pc-/-] (a) (scale bar 50 μm). Blue=nuclear hemalaun counterstaining, red=Ki67 nuclear + cytoplasm. Ki67 activity of PTEN[pc+/-]cJun[pc+/-]JunB[pc-/-]was lower compared to wt and cre+ PTEN[pc+/-] (b).

7.4. Western blot analysis

We analyzed expression levels of total prostate tissue by western blot of wt, PTEN$^{pc+/-}$, and PTEN$^{pc-/-}$ (n=3 each).

No differences were recognized in the expression of AR in wt compared to PTEN$^{pc-/-}$. In PTEN$^{pc+/-}$ AR activation was increased in PTEN$^{pc-/-}$ compared to wt. In accordance with the datasheet of the AR antibody the bands for the AR should be seen at 110 kDa but they were recognized at 160 kDa.
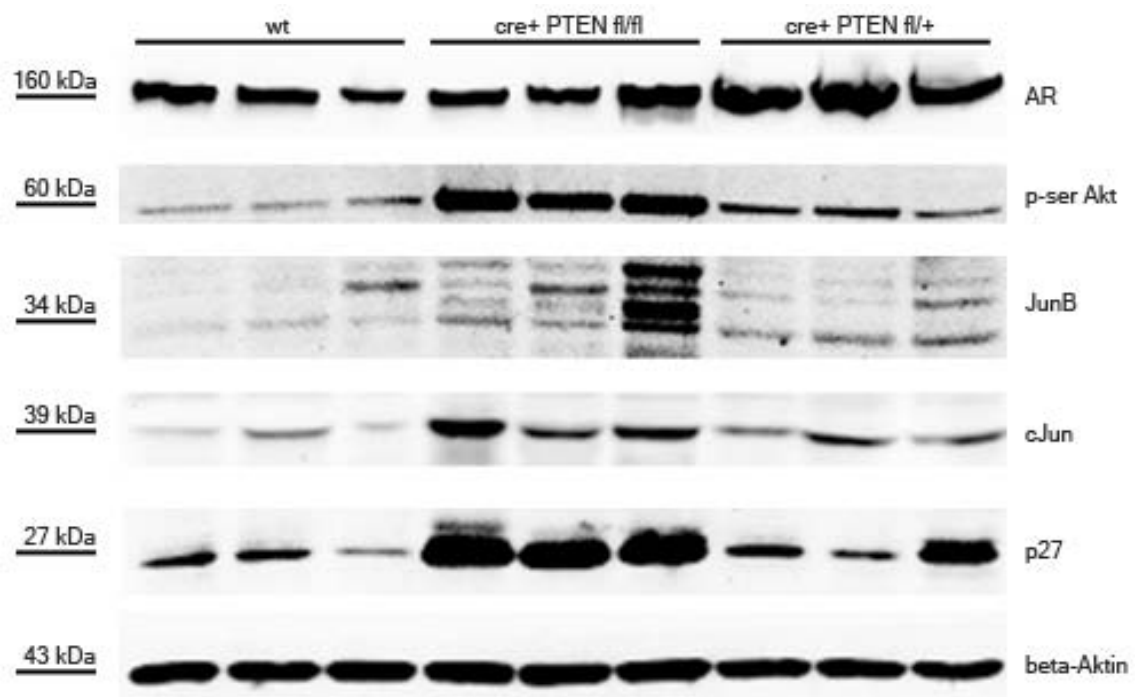
Figure 37: Picture of WB with 3 different samples per genotype. Loading control was beta Actin. Side note: Beta-actin, JunB and cJun bands shown have not been taken from the same blot, yet from blots with same concentrations. This collage was necessary, as these three proteins could not be distinguished on one blot.

The WB was repeated several times with the same result. Because of this discrepancy in molecular weight the results of AR expression should be evaluated critically. In this case the IHC of the AR is more meaningful.

JunB and cJun expression was lowest in wt prostates. In PTEN$^{pc+/-}$ the JunB and cJun expression was slightly elevated but in PTEN$^{pc-/-}$ it was highly increased.

Similarly, p27 expression was increased in PTEN$^{pc-/-}$ compared to wt and PTEN$^{pc+/-}$ prostates.

For p-serAkt expression an increased expression in PTEN[pc+/-] to PTEN[pc-/-] compared to wt was seen (Figure 37).

The expression of p16 and p65 was higher in PTEN[pc-/-] compared to wt. However, the tumor suppressor p53 was expressed at a higher level in wt than in PTEN knock out prostate tissue (Figure 38).
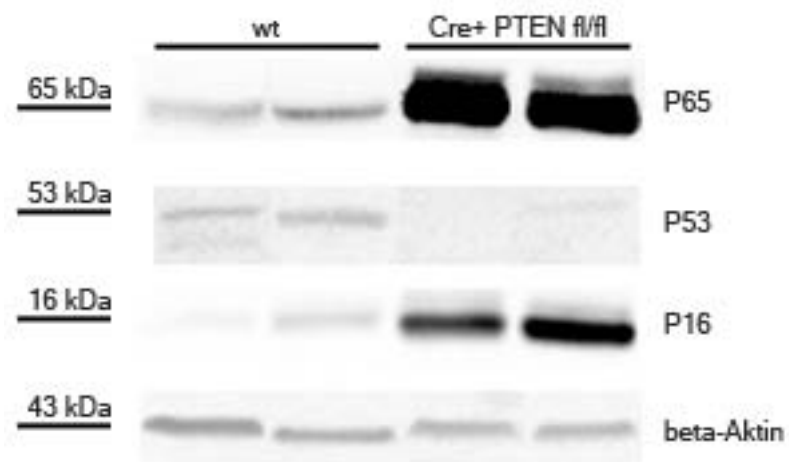
Figure 38: Picture of WB with 2 different samples per genotype. Loading control was beta Actin. Side note: Beta-actin, P53 and P65 bands have been taken from different blots using equal sample concentrations.

8. Discussion

The effects of cJun and JunB on cancer range from tumor suppressor to oncogenic action. In PCa their role is discussed controversially. To better understand the influences of these two AP1 members on PCa we took advantage of a PCa mouse model (PTEN$^{pc-/-}$) where we also did an additional knockout of cJun and/or JunB.

In this master thesis we tried to get genotypes for PTEN$^{+/-}$, PTEN$^{pc-/-}$, PTEN$^{pc-/-}$cJun$^{pc-/-}$JunB$^{pc-/-}$, PTEN$^{pc-/-}$cJun$^{pc-/-}$JunB$^{pc+/+}$, PTEN$^{pc-/-}$cJun$^{pc+/+}$JunB$^{pc-/-}$.

The first attempted breeding was successful. Prostates of the PTEN$^{pc-/-}$ showed the expected enlargement due to the massive tumor development. Mice with the genotype of wt and PTEN$^{pc+/-}$ showed a normal macroscopic prostate and the weight of the prostate in both genotypes was significantly smaller as compared to PTEN$^{pc-/-}$. Values indicated by C_v were representative.

The second generation was showing problems in the genotype. During this breeding female cre+ PTEN fl/fl and male cre- cJun fl/fl JunB fl/fl were crossed. Female cre+ PTEN fl/fl were used for this breeding since males with this genotype are usually unable to breed due to proceeding PCa.
Instead of the expected genotype PTEN fl/+ in the first generation PTEN Δ/+ genotypes occurred in the entire brood. For cJun and JunB not only fl/+ but also fl/fl and +/+ was observed in the offspring.
An explanation for this phenomenon could be that during the breeding with PB-Cre4 mice small foci of expression of Cre were seen not only in the specific tissue but also in seminal vesicals, testis and ovaries. In contrast to the testicular expression, the Cre expression in the ovaries has an influence on the floxed alleles. It has been shown that in cre+ females, oocyte mediated recombination can occur [WU et al., 2001].

This recombination would explain the Δ PTEN allele in mice at 3-4 weeks of age. One allele of the PTEN gene is already excised in embryogenesis. Whether the genotypes of cJun and JunB are possibly also explainable with the PB-Cre4 females remains unclear.

There are different options to solve this PTEN breeding problem. One could try to use male cre+ PTEN fl/fl mice for the breeding as soon as possible before they become infertile within approximately 12 weeks. Another option is to cross male cre+ PTEN fl/+ mice with female cre- cJun fl/fl JunB fl/fl mice. The advantage is that male mice become infertile only after approximately 9 months and can therefore have more offspring. On the other hand this breeding pattern takes more time to produce the desired genotype. In contrast to the first breeding method only some mice will manifest PTEN fl/+,which is the desired genotype for the next breeding to achieve the final genotype of PTEN fl/fl with cJun, JunB double or single knock out.

There are alternative methods for prostate specific Cre activity available. A relatively new method is to use an inducible Probasin Cre.
The advantage is that the researcher can choose the moment to induce the Cre. This is useful in the case of prostate cancer because this is a disease mainly occurring in elderly men. Instead of the PB-Cre4 that is already active in the young adult, the inducible Cre can be activated in older mice. Birbach et al. developed a mouse line expressing an inducible Cre protein (MerCreMer).This Cre is controlled by regulatory elements of the Probasin gene on a bacterial artificial chromosome (BAC). The induction of the MerCreMer occurs via Tamoxifen. The Cre shows a high controllability and no background recombination [BIRCHBACH et al., 2009].
Therefore it seems that the inducible Cre could be the solution to the breeding problems caused by the imprinting of the Probasin gene mentioned above.

To get at least some insight on the issue whether cJun and JunB work as tumor suppressors or inducers, the cJun and JunB knockouts with the following genotypes were analyzed:
1. PTEN$^{pc+/-}$cJun$^{pc+/-}$, 2. PTEN$^{pc+/-}$cJun$^{pc-/-}$JunB$^{pc+/-}$ and 3. PTEN$^{pc+/-}$cJun$^{pc+/-}$JunB$^{pc-/-}$ and appropriate controls.

Some unexpected observations were made in PTEN$^{pc+/-}$cJun$^{pc-/-}$JunB$^{pc+/-}$ prostates. These mice developed a histological pronounced PCa. Since the histology of PTEN$^{pc+/-}$cJun$^{pc+/-}$JunB$^{pc-/-}$ was similar to PTEN$^{pc+/-}$prostates, the loss of one additional cJun allele

seems to accelerate tumor development. Therefore we assume that cJun might act as a tumor suppressor in the prostate. Ongoing experiments in the lab using PTEN$^{pc-/-}$ cJun$^{pc-/-}$ should be able to elucidate this question.

An interesting new analysis of Walker and Kennedy supports the idea of cJun acting as a tumor suppressor in PCa. They analyzed a human prostate online dataset of Taylor et al. (Cancer Cell 2010) with regard to the role of cJun expression in human PCa patients. Using a Kaplan-Meier analysis of survival, PCa patients with cJun loss were compared to PCa patients with cJun expression. The loss of cJun in PCa showed a highly significant decrease in the survival rate as compared to PCa patients with cJun expression (Hazard ratio: 11.2, p < 0.0001) (WALKER S and KENNEDY R., unpublished data).

We were interested in looking at the protein expression profiles of AR, cJun, JunB and Ki67 in genotypes that were available at the time.
AR-expression was highest in PTEN$^{pc-/-}$, intermediate in PTEN$^{pc+/-}$and lowest in the wt prostate samples. The expression of the AR obviously increases with the progression of the tumor. In the PTEN$^{pc+/-}$cJun$^{pc-/-}$JunB$^{pc+/-}$ mice the expression of the AR was even a little higher than in PTEN$^{pc-/-}$. This result is interesting, because in cJun$^{pc-/-}$ only one allele of PTEN was knocked out, supporting the idea of cJun acting as a tumor suppressor.
Ki67, a nuclear protein that is active in cellular proliferation, was also analyzed and its expression was also high in PTEN$^{pc-/-}$, it decreased in PTEN$^{pc+/-}$ and was lowest in the wt prostate samples. Interestingly, Ki67 expression was also higher in the PTEN$^{pc+/-}$cJun$^{pc-/-}$ JunB$^{pc+/-}$ mice compared to the other groups.
The PTEN$^{pc+/-}$cJun$^{pc+/-}$JunB$^{pc-/-}$ sample showed the lowest Ki67 activity supporting the observation that loss of JunB has little influence on PCa development.
Taken together the results of the HE stainings and the IHC for AR and Ki67 indicate that the knockout of cJun increases the tumor development in PCa.

Summarizing the results for the HE-stainings, Ki67 -and AR-staining the PTEN$^{pc+/-}$cJun$^{pc+/-}$JunB$^{pc-/-}$ are comparable to PTEN$^{pc+/-}$ prostates and it seems that a JunB

knockout does not increase the tumor development, in contrast to PTEN$^{pc+/-}$cJun$^{pc-/-}$ JunB$^{pc+/-}$ prostate, where we could see increased tumor development.

For a better understanding of the previous data, also cJun and JunB expression profiles were established with IHC.
The JunB expression is increasing from wt over PTEN$^{pc+/-}$ to PTEN$^{pc-/-}$ prostates. For cJun almost no expression was detected in the wt and PTEN$^{pc+/-}$ prostate samples but in PTEN$^{pc-/-}$ a high increase in cJun expression was observed.

This increase of cJun and JunB expression from normal prostate tissue to prostate tumor tissue was also seen in the expression of AR and Ki67. These findings correlate with the JunB expression profiles by the previously presented study of Chandran et al. (increase of expression from wt to primary prostate tumors) but they differ considerably from the JunB expression in prostates established by Li et al., which showed a decrease in expression from normal prostate tissue to progressive PCa.
One explanation for these differing results in expression profiles of prostate tissue could be an altered expression of specific genes after surgical interventions. A study of Lin et al. showed that the expression of genes like cJun and JunB can be increased after surgical manipulation of the prostate. An in situ prostate biopsy in patients with clinically localized prostate cancer showed low levels of cJun and JunB expression. Subsequent to this in situ biopsy a radical prostatectomy was performed and immediately after this surgical removal an ex vivo biopsy showed highly increased expression levels of cJun and JunB. The explanation for this observation is a stress induced activation of the JNK pathway. cJun and JunB are direct targets of this pathway and they seem to be activated by this JNK stress-response pathway. However, the size of the prostate is a limiting factor. Lin et al. showed that the difference in gene expression between in vivo and ex vivo biopsies decreases when the size of the prostate increases [LIN et al. 2006].
The study of Lin et al. showed that the method of providing the prostate tissue as well as the prostate size can influence the prostate gene expression. In the case of Chandran et al. different methods for providing the different prostate tissues were

accomplished and their expression profiles might be influenced by the different methods utilized. In our case all mice prostates, regardless of the genotype, were treated the same way. In consideration of the study of Lin et al. the expression of genes like cJun and JunB should be increased not only in the prostate tumor tissue but also in the normal prostate tissue because of the same activation by JNK stress response. This problem did not occur within mice prostate samples of this thesis since all samples were prepared the same way.

Puhr et al. demonstrated that the expression of the AP-1 members cJun and JunB inversely correlate to the expression of the AR in different human prostate cell lines. This does not support our findings, specifically the positive correlation in the expression profiles of cJun, JunB and AR in mouse prostates observed in this thesis. In the mouse prostates cJun, JunB and AR expression increase from normal prostate tissue to PCa tissue. Possibly the results are not comparable in this case because of the different conditions between cell culture experiments and mouse models.

Jin et al. found that a PTEN knock out in breast cancer cell lines activates cJun and JunB by unsuppressing the MAPK-pathway and further the JNK-pathway. This is another possible explanation for the increase of cJun and JunB in the PTEN knock-out mice compared to the wt [JIN et al., 2008].

As has been mentioned in the literature before, an increased level of JunB and especially of cJun in different tumors often correlates with their function as oncogenes. If this was the case in PCa, the knockout of cJun and JunB in mouse PCa should cause some tumor suppressive effects or at least no additional tumorigenic effects. Our findings showed that a knockout of cJun even drives the tumor development. This observation suggests that cJun might have tumor suppressor activities in the prostate. The knockout of JunB in the mouse prostate does not give such clear results but it has to be mentioned again that the analysis of one JunB knockout mouse can only give a rough idea of the involved processes, it is impossible to make meaningful conclusions.

The overexpression of cJun in PTEN$^{pc-/-}$ mice might indicate that the tumor suppressor effects of cJun are suspended or covered up by other mechanisms.

Another interesting observation was made concerning the cJun and JunB expression profile. In the PTEN$^{pc+/-}$cJun$^{pc-/-}$JunB$^{pc+/-}$genotype the JunB expression was increased massively. On the other hand, in the PTEN$^{pc+/-}$cJun$^{pc+/-}$JunB$^{pc-/-}$ the cJun expression was greatly increased.

It seems that cJun and JunB might be able to substitute for each other if one component is knocked out.
It was described that JunB is able to substitute for the absence of cJun by a transgenic complementation approach and a knock-in strategy. In the embryonic development JunB knock-in can compensate the lack of cJun and prevents cardiac and liver defects, which usually occur in absence of cJun [Passegué et al., 2002].

WB-analysis was done to confirm the results of the IHC with focus on cell cycle protein expression.
For cJun and JunB the results of Western Blotting confirm the results of the IHC-analysis. An increase in protein expression was observed in wt compared to PTEN$^{pc+/-}$ compared to PTEN$^{pc-/-}$. It seems that the expression of cJun and JunB increases the more prostate tumor progression occurs.
Finally WB-analysis was done for p65, p53, p27, p16 and p-ser Akt. Alterations in the expression of these proteins play an important role in tumor progression. cJun and JunB are able to influence the cell cycle [PIECHACZYK and FARRAS, 2008]. With the measurements of these proteins it might be possible to get some more information about the influence of cJun and JunB in the tumor progression of PCa.

The expression of the tumor suppressor p53 is decreased in the prostate tumor samples compared to the wildtype samples. This decrease is often observed in tumor development and one reason for the increased proliferation in tumor tissue. The increased levels of cJun in the prostate tumor tissue can influence the p53 expression, because, as it was mentioned before, cJun negatively regulates p53 by directly binding to the promoter region of p53 [SHAULIAN and KARIN, 2002].

p27, a CDK-inhibitor mediates cell cycle arrest in G1 and thereby negatively regulates cell proliferation. The expression of p27 increased from wildtype compared to PTEN[pc+/-] compared to PTEN[pc-/-]. Studies from 1999 analyzing the expression of p27 in PCa showed different results. Fernandez et al., found a decreased expression of p27 in human PCa progression [FERNANDEZ et al., 1999]. Agus et al. also observed a low expression of p27 in prostate cancer cells, but a massive increase of expression was recognized after androgen withdrawal. The degradation of p27 in PCa seems to be androgen dependent [AGUS et al., 1999]. Therefore an androgen withdrawal experiment in the PTEN[pc-/-] mice would be interesting.

The crosstalk between the stroma and the epithelium of the prostate plays another important role in PCa development.

Stromally expressed cJun in fibroblasts is able to influence the expression of p27 in prostate epithelial cells. cJun increase the production of IGF-1 in the stroma. IGF-1 was shown to upregulate the epithelial protein level of Akt, Cyclin D1 and MAPK whereas the p27 protein level is decreased. This cJun dependent IGF-1 production causes benign prostate hyperplasia-1 (BPH-1) cellular proliferation [LI et al., 2007].

These results are in contrast to the expression profile of p27 we found in PTEN[pc-/-] mice. The protein level of p27 should also be analyzed by IHC, because with this method it is possible to specifically analyze prostate epithelial cells.

The expression of the tumor suppressor p16 is increased in the PTEN[pc-/-] prostate tumor tissue compared to the normal prostate tissue.

In 1997, Halvorsen et al. also found an overexpression of p16 in the majority of prostate adenocarcinomas compared to hyperplastic or normal prostate glands. Explanations for this overexpression were rare. The frequency of point mutations of the p16 gene was analyzed, because mutations in critical genes play an important role in tumorigenesis in many other cancer types. For p16 a very low frequency of point mutations was detected and therefore cannot be used as an explanation for the overexpression. Other mechanisms, like the inactivation by methylation of the p16 gene, were observed more frequently [HALVORSEN et al., 1997].

cJun, which shows a higher expression in the tumor tissue, might be one regulator of p16(INK4a) in the prostate tissue. In 2011, Kollmann et al. discovered that cJun is able to prevent the methylation of p16 (INK4a). cJun stops the epigenetic silencing of the gene by binding to the promoter region and thereby precludes methylation of p16(INK4a) [KOLLMANN et al., 2011].

The expression pattern of JunB might be another explanation for the high expression of p16 in the prostate tumor tissue. It upregulates p16 and leads to dephosphorylation of pRb. In transient amplifying cells (basal cell population of the prostate epithelium) this mechanisms leads to senescence. If JunB is downregulated in these cells the level of p16 decreases and the cells are able to bypass senescence and proliferate again [KONISHI et al., 2008].

The protein kinase Akt was also analyzed because Akt is able to inhibit apoptosis and thereby promotes cell survival and it is negatively regulated by PTEN. The expression of Akt increased from wildtype to PTEN$^{pc-/-}$, which is not surprising on first sight. However, cJun probably also plays a role in Akt activation. As was mentioned before Li et al. showed that stromally expressed cJun in fibroblasts activates IGF-1 and thereby upregulates epithelial protein level of Akt [LI et al., 2007].

NFκB deregulation has often been observed in cancer progression. In many types of cancer including PCa NFκB expression is increased. To investigate the expression of NFκB in the used mouse model, p65 antibody, a subunit of NFκB, was used. The expression of p65 increased in PTEN$^{pc-/-}$ compared to the wildtype prostate tissue. Little is known about direct mechanisms of AP-1 that modulate the NFκB-pathway. In a study of Sanchez-Perez in 2002 a crosstalk between cJun and NFκB was observed. The chemotherapeutic agent cisplatin induces apoptosis via activation of JNK-pathway. In cisplatin treated human embryonic kidney fibroblasts cJun is able to inhibit NFκB, thereby inducing apoptosis. Cisplatin treated fibroblasts with cJun -/- showed no inhibition of NFκB and lead to cell survival [SANCHEZ-PEREZ et al., 2002].

Taken together, many of the observations made in the experiments of this master thesis support the idea of cJun acting as a tumor suppressor. For JunB the results do

not show such clear tendency. A relationship between the AR and cJun, JunB seen in the data of Puhr et al. could not be confirmed.

9. Conclusion

In this master thesis a PB-Cre4 (PTEN$^{pc-/-}$) mouse model was used to analyze the effect of cJun and JunB in PCa. cJun and JunB knockout strains were inbred to increase the amount of information.

In the breeding of PB-Cre4 females with male cJun fl/fl JunB fl/fl various problems with the resulting genotypes occurred. This was probably due to the oocyte mediated recombination using female PB-Cre4 mice [WU et al 2001]. In further studies male PB-Cre4 mice might be used and crossed as soon as possible before they become infertile. If this method does not show the predicted outcome an inducible Cre as described by Birbach et al. would be another option to achieve the volitional genotypes.

The first aim of this master thesis was to describe the effects of cJun and JunB in PCa. After analyzing all results it seems that cJun acts as tumor suppressor in PCa. The tumor development was equal or even more pronounced in prostates with cJun knocked out as compared to prostates with only a PTEN knockout (PTEN$^{pc+/-}$cJun$^{pc-/-}$ JunB$^{pc+/-}$ vs. PTEN$^{pc-/-}$) although in the cJun knockout mice only one allele of PTEN was knocked out. It will be interesting to see the tumor development in the genotype of PTEN$^{pc-/-}$cJun$^{pc-/-}$ in further studies. The expression of Ki67 and the AR was also increased in PTEN$^{pc+/-}$cJun$^{pc-/-}$JunB$^{pc+/-}$ as compared to PTEN$^{pc-/-}$. The upregulated cJun activity in PTEN$^{pc-/-}$ might be due to its tumor suppressor function that is suspended or covered up by other mechanisms.

For JunB the results showed neither a tumor suppressor nor an oncogenic function in PCa. The knockout of JunB in the PTEN mouse model showed no change in the tumor development. In Ki67 and AR expression no change was observed compared to wt and PTEN$^{pc+/-}$.

Another interesting observation concerning the relationship of cJun and JunB was made when cJun or JunB were knocked out. It seems that cJun and JunB can compensate for each other. In case of a cJun knock out, the JunB expression increased opposed to an increase in a cJun transcription when JunB was knocked out.

The second aim was to find out whether or not cJun, JunB and the AR can influence each other. After analyzing all data, no direct effect of cJun, JunB on the AR or vice versa was observed. The data of Puhr et al., reporting inverse expression of cJun/JunB and the AR could not be confirmed.

Summarizing, the most promising observation in this master thesis was the tumor suppressor function of cJun in PCa in mouse models. This effect should be analyzed in further experiments especially with the additional genotypes that were missing in this thesis ($PTEN^{pc-/-}cJun^{pc-/-}JunB^{pc-/-}$, $PTEN^{pc-/-}cJun^{pc-/-}JunB^{pc+/+}$, $PTEN^{pc-/-}cJun^{pc+/+}JunB^{pc-/-}$). It would be interesting to understand the mechanisms behind the tumor suppressor function of cJun in more detail. One suggestion would be to do further analysis of the stromal epithelial crosstalk. Another interesting point would be to generate $PTEN^{pc-/-}$ $cJun^{pc-/-}$ and/or $JunB^{pc-/-}$ cell lines when the breeding was successful. With these cell lines more and easier experiments could be done including cell cycle experiments using FACS analysis.

10. References

AGUS DB, CORDON-CARDO C, FOX W, DROBNJAK M, KOFF A, GOLDE DW, SCHER HI. Prostate Cancer Cell Cycle Regulators: Response to Androgen Withdrawal and Development of Androgen Independence. J Natl Cancer Inst. 1999; 91: 1869-1876.

BERG D, HIPP S, MALINOWSKY K, BÖLLNER C, BECKER KF. Molecular profiling of signaling pathways in formalin-fixed and paraffin-embedded cancer tissues. Eur J Cancer 2010; 46: 47-55.

BIRBACH A, CASANOVA E, SCHMID J. A Probasin MerCreMer BAC Allows Inducible Recombination in the Mouse Prostate. Genesis 2009; 47: 757-764.

BRAY F, REN JS, MASUYER E, FERLAY J. Global Estimates of Cancer Prevalence for 27 Sites in the Adult Population in 2008. Int J Cancer 2012; DOI: 10.1002/ijc.27711.

CANNATA D, KIRSCHENBAUM A, LEVINE A. Androgen Deprivation Therapy as Primary Treatment for Prostate Cancer. J Clin Endocrinol Metab 2012; 97: 360-365.

CHANDRAN U, MA C, DHIR R, BISCEGLIA M, LYONS-WEILER M, LIANG W, MICHALOPOULOS G, BECICH M, MONZON F. Gene Expression Profiles of Prostate Cancer Reveal Involvement of Multiple Molecular Pathways in the Metastatic Process. BMC Cancer 2007; 7:64.

CHEN S-Y, CAI C, FISHER CJ, ZHENG Z, OMWANCHA J, HSIEH C-L, SHEMSHEDINI L. c-Jun enhancement of androgen receptor transactivation is associated with prostate cancer cell proliferation. Oncogene 2006; 25: 7212-7223.

CURRAN S, AKIN O, AGILDERE AM, ZHANG J, HRICAK H, RADEMAKER J. Endorectal MRI of Prostatic and Periprostatic Cystic Lesions and their Mimics. AJR Am J Roentgenol 2007; 188: 1373-1379.

EFERL R, WAGNER E. AP-1: A Double Edged Sword in Tumorigenesis. Nat Rev Cancer 2003; 3: 859-868.

FELDMANN B, FELDMANN D. The Development of Androgen-Independent Prostate Cancer. Nat Rev Cancer 2001; 1: 34-45.

FERNANDEZ PL, ARCE Y, FARRÉ X, MARTÍNEZ A, NADAL A, REY MJ, PEIRÓ N, CAMPO E, CARDESA A. Expression of p27/kip1 is down-regulated in human prostate carcinoma progression. J Pathol 1999; 187: 563-566.

EPSTEIN JI, ALLSBROOK WC, AMIN MB, Egevad LL, ISUP Grading Committee. The 2005 International Society of Urological Pathology (ISUP) Consensus Conference on Gleason Grading of Prostatic Carcinoma. Am J Surg Pathol 2005; 29: 1228-1242.

FREEDLAND S. Screening, Risk Assessment, and the Approach to Therapy in Patients with Prostate Cancer. Cancer 2011; 117: 1123-1135.

HALVORSEN OJ, HAUKAAS S, HOISAETER P, AKSLEN L. Expression of p16 Protein in Prostatic Adenocarcinomas, Intraepithelial Neoplasia, and Benign/Hyperplastic Glands. Urol Oncol 1997; 3: 59-66.

HEEMERS H, TINDALL D. Androgen Receptor (AR) Coregulators: A Diversity of Functions Converging on and Regulating the AR Transcriptional Complex. Endocr Rev 2007; 28: 778-808.

HOFFMANN R. Screening for Prostate Cancer. N Engl J Med 2011; 365: 2013-2019.

HOLLANDER MC, BLUMENTHAL G, DENNIS P. PTEN Loss in the Continuum of Common Cancers, Rare Syndromes and Mouse Models. Nat Rev Cancer 2011; 11:289-301.

JIN Y, HU JL, XIAO L, CUI W. Impact of PTEN knockout in human breast carcinoma MCF-7 cells on activity of JNK pathway. Chin J Cancer 2008; 27: 490-493.

JOCHUM W, PASSEGUÉ E, WAGNER E. AP-1 in mouse development and tumorigenesis. Oncogene 2001; 20: 2401-2412.

JOHNSON M, HERNANDEZ I, WEI Y, GREENBERG N. Isolation and Characterization of Mouse Probasin: An Androgen-Regulated Protein Specifically Expressed in the Differentiated Prostate. The Prostate 2000; 43: 255-262.

KASPER S. Survey of Genetically Engineered Mouse Models for Prostate Cancer: Analyzing the Molecular Basis of Prostate Cancer Development, Progression and Metastasis. Journal of Cellular Biochemistry 2005; 94: 279-297.

KOLLMANN K, HELLER G, SEXL V. c-Jun prevents methylation of p16^{INK4a} (and CDK6): the villain turned bodyguard. Oncotarget 2011; 2: 422-427.

KONISHI N, SHIMADA K, NAKAMURA M, ISHIDA E, OTA I, TANAKA N, FUJIMOTO K. Function of JunB in Transient Amplifying Cell Senescence and Progression of Human Prostate Cancer. Clin Cancer Res 2008; 14: 4400-4407.

KOOCHEKPOUR S. Androgen Receptor Signaling and Mutations in Prostate Cancer. Asian J Androl 2010; 12: 639-657.

LIN DW, COLEMAN IM, HAWLEY S, HUANG CY; DUMPIT R, GIFFORD D, KEZELE P, HUNG H, KNUDSEN BS, KRISTAL AR, NELSON PS. Influence of Surgical Manipulation on Prostate Gene Expression: Implications for Molecular Correlates of Treatment Effects and Disease Prognosis. J Clin Oncol 2006; 24: 3763-3770.

LI B, TOURNIER C, DAVIS R, FLAVELL R. Regulation of IL-4 expression by the transcription factor JunB during T helper cell differentiation. The EMBO Journal 1999; 18: 420-432.

LI W, WU C-L, FEBBO P-G, OLUMI AF. Stromally Expressed c-Jun Regulates Proliferation of Prostate Epithelial Cells. Am J Pathol.2007; 171: 1189-1198.

MENG Q, XIA Y. c-Jun, at the Crossroad of the Signaling network. Protein Cell 2011; 2: 889-898.

NIU YN, XIA SJ. Stroma-epithelium crosstalk in prostate cancer. Asian J Androl 2009; 11: 28-35.

PASSEGUÉ E, JOCHUM W, BEHRENS A, RICCI R, WAGNER E. JunB can substitute for Jun in mouse development and cell proliferation. Nat Genet 2002; 30: 158-166.

PIECHACZYK M, FARRAS R. Regulation and function of JunB in Cell Proliferation. Biochem Soc Trans 2008; 36: 864-867.

RICOTE M, ROYUELA M, GARCIA-TUNON I, BETHENCOURT F, PANIAGUA R, FRAILE B. Pro-apoptotic Tumor Necrosis Factor-α Transduction Pathway in Normal Prostate, Benign Prostatic Hyperplasia and Prostatic Carcinoma 2003; 170: 787-790.

ROSS J. The Androgen Receptor in Prostate Cancer: Therapy Target in Search of an Integrated Diagnostic Test. Adv Anat Pathol 2007; 14: 353-357.

SANCHEZ-PEREZ I, BENITAH SA, MARTINEZ-GOMARIZ M, LACAL JC, PERONA R. Cell Stress and MEKK1-mediated c-Jun Activation modulate NFκB Activity and Cell Viability. Mol. Biol. Cell 2002; 13: 2933-2945.

SHAPPELL S, THOMAS G, ROBERTS R. Prostate Pathology of Genetically Engineered Mice: Definitions and Classification. The Consensus Report from the Bar Harbour Meeting of the Mouse Models of Human Cancer Consortium Prostate Pathology Committee. Cancer Res 2004; 64: 2270-2305.

SHAULIAN E. AP-1 – The Jun Proteins: Oncogenes or Tumor Suppressors in Disguise? Cellular Signaling 2010; 22: 894-899.

SHAULIAN E, KARIN M. AP-1 as a Regulator of Cell Life and Death. Nat Cell Biol. 2002; 4: E131-136.

STATISTIK AUSTRIA. Gesundheit. In: Statistisches Jahrbuch Österreichs 2012. Verlag Österreich GmbH, 2011; 119.

STRICKLETT P, NELSON R, KOHAN D. The Cre/loxP System and Gene Targeting in the Kidney. Am J Physiol Renal Physiol 1999; 276: F651-F657.

THOMPSON I, TRASHER JB, AUS G, BURNETT AL, CANBY-HAGINO ED, COOKSON MS, D'Amico AV, DMOCHOWSKI RR, ETON DT, FORMAN JD, GOLDENBERG SL, HERNANDEZ J, HIGANO CS, KRAUS SR, MOUL JW, TANGEN CM. Guideline for the Treatment of Clinically Localized Prostate Cancer: 2007 Update. J Urol 2007; 177: 2106-2131.

TINIAKOS D, MITROPOULOS D, KYROUDI-VOULGARI A, SOURA K, KITTAS C. Expression of c-Jun Oncogene in Hyperplasia and Carcinomatous Human Prostate. Urology 2006; 67: 204-208.

VESELY P, STABER P, HÖFLER G, KENNER L. Translational Regulation Mechanisms of AP-1 Proteins. Mutat Res 2009: 682; 7-12.

WU X, WU J, HUANG J, POWELL W, ZHANG JF, MATUSIK R, SANGIORGI F, MAXSON R, SUCOV H, ROY-BURMAN P. Generation of a Prostate Epithelial Cell-Specific Cre Transgenic Mouse Model for Tissue-Specific Gene Ablation. Mech Dev 2001, 101: 61-69.

YAMAOKA M, HARA T, KUSAKA M. Overcoming Persistent Dependency on Androgen Signaling after Progression to Castration-Resistant Prostate Cancer. Clin Cancer Res 2010; 16: 4319-4324.

YUAN H, YOUNG C, TIAN Y, LIU Z, ZHANG M, LOU H. Suppression of the Androgen Receptor Function by Quercetin through Protein-Protein Interactions of Sp1, c-Jun and the Androgen Receptor in Human Prostate Cancer Cells. Mol Cell Biochem 2010; 339: 253-262.

Curriculum vitae

personal details

name:	Nora Dzuck
address:	Rebenweg 28, 8610 Uster
phone:	+ 41 78 66 88 300
email:	nora.dzuck@gmx.de
birth date and place:	August 10th, 1984 in Dresden, Germany
marital status:	spouse, one daughter
nationality:	German
parents:	Holger Dzuck, lathe operator
	Annette Dzuck, secretary
sibling:	Phillipp Dzuck, nurse

primary and secondary education

June 2003	Abitur - school leaving certificate with focus on Biology and German
1995 – 2003	Fritz-Löffler-Gymnasium in Dresden, Germany
1991 – 1995	47. Grundschule in Dresden, Germany

tertiary education

since September 2010	research assistant with focus on prostate cancer in the Prof. Kenner group at the Department of Pathology and Histology at the Medical University of Vienna, Austria – including a scientific thesis titled: „Effects of cJun and JunB on Prostate Cancer"
since October 2008	studying in the masters program of nutritional science at the University of Vienna, Austria
October 2008	Bachelor of science in nutritional science
March 2005 – October 2008	studying in the bachelors program of nutritional science at the University of Vienna, Austria

further experiences and qualifications

July 2010 – August 2010	employment as assistant in the private practice for complementary medicine and anti-aging Dr. Liebscher in Dresden, Germany
March 2004 – February 2005	launching and managing the café "Unico" in Dresden, Germany
September 2003 – June 2004	employment as assistant in the orthopedic practice Leipziger Strasse in Dresden, Germany
since 1998	competitive floorball career with various league participations in Germany and Austria, german national U-19 and A-team player from 2000 to 2003

language skills

German – native
English – proficient, both verbal and written